

Supergen



Offshore
Renewable
Energy

Early Career Researcher Posters and Abstracts Booklet

2024 Annual Assembly:
Accelerating Offshore Renewable
Energy to 2040 and beyond



Engineering and
Physical Sciences
Research Council

Early Career Researcher Posters 2024

Please note - some authors have only provided a poster or abstract.

Poster title and Author
Characterisation of Structured Natural Rubber for Enhanced Performance in Oscillating Water Column Wave Energy Converters - Dr Farhad Abad
Hinged very large floating structures for wave energy conversion and wind turbine foundation - Dr Abel Arredondo-Galeana
Soil Reaction Curves for the Response of Monopile Tip in Clay - Abigail Bateman
Durability of polymer composite materials for ORE applications - Dr Jasmine Bone
Estimating Wind Using Wave Buoy Measurement: A case study in the Celtic Sea - Dr Jiaxin Chen
CoTide: Multi-rotor utility-scale Tidal Energy Concepts - Dr Xiaosheng Chen
Interpreting the ALPACA lateral pile load tests results: modelling accumulated displacements in chalk - Dr Jamie Crispin
Optimisation of the geometry of a top-hinged wave energy converter - Dr Emma Edwards
LES of Wind Farms with DOFAS: Sensitivity to the SGS Model - Mina Ghobrial
Variable amplitude fatigue testing of large-scale high strength steel cast node tubular connections - John Harris
A sea-state-dependent power-limiting control strategy for wave energy converters - Dr Zhijing Liao
Controlling turbine tip vortices and cavitation through local permeability - Dr Yabin Liu
Numerical and Experimental Assessment of a Floating Offshore Wind Turbine platform for hydrogen production and storage - Dr Claudio Rodriguez Castillo
A Control Centred Approach for Off-Grid Green Hydrogen Production from Wind Energy - Researcher in Residence Scheme Project - Dr Adam Stock
Thermal Boundary Layer around a Partially Buried Pipe in Oscillating Flow - Henry Thomas
Short design wave and wind events for Spar type FOWTs in idling conditions - Tom Tosdevin
An Origami-Inspired Wave Energy Converter through Direct Energy Generation - Dr Jingyi Yang
Numerical Analysis of Axially Loaded Wind Turbine Jacket Piles in Chalk - Dr Miad Saberi
Cost Optimisation of Offshore Wind Farm Combination with reversible Solid Oxide Cell System Producing Hydrogen using the PyPSA Power System Modelling Tool - Dr Jessica Guichard
Short design waves for predicting extreme responses of floating ORE devices - Dr Scott Brown

Characterisation of Structured Natural Rubber for Enhanced Performance in Oscillating Water Column Wave Energy Converters

Farhad Abad*, Guillermo Idarraga Alarcon, Saeid Lotfian, Liu Yang, Saishuai Dai, Yang Huang, Qing Xiao, Feargal Brennan

Faculty of Engineering, University of Strathclyde, Glasgow G4 0LZ, UK
University of Strathclyde, Glasgow, UK

*Corresponding author: Email: farhad.abad@strath.ac.uk

Abstract

The study introduces the novel idea of using structured natural rubber, resembling Auxetic patterns, in Oscillating Water Column (OWC) Wave Energy Converters (WECs). These membranes exhibit a non-linear stiffness that increases with higher pressure in the air chamber and harsh environmental conditions. They also exhibit differing behaviours depending on the deformation mode. To accurately capture their responses, bulge testing is employed, simulating the deformation mode within OWC devices. This novel idea is combined with a sophisticated characterisation technique to find homogenised hyperelastic models [1]. The study aims to enhance OWC efficiency and reliability by identifying optimised membrane geometries and properties. Moving forward, model refinement and further experiments will validate findings and drive progress in this field. Our future work will use the obtained hyperelastic models in fluid-structure interaction simulations of structured membranes in OWCs.

Keywords: Structured membrane; OWC; Material Characterisation; Inflatable diaphragm; Dry test rig.

References

1] Abad, F., Lotfian, S., Dai, S., Zhao, G., Alarcon, G.I., Yang, L., Huang, Y., Xiao, Q. and Brennan, F., 2024. Experimental and computational analysis of elastomer membranes used in oscillating water column WECs. *Renewable Energy*, p.120422.

Characterisation of Structured Natural Rubber for Enhanced Performance in Oscillating Water Column Wave Energy Converters

Bionic Adaptive Stretchable Materials for Wave Energy Converters (BASM-WEC)

Farhad Abad*, Guillermo Alarcon, Saeid Lotfian, Liu Yang, Saishuai Dai, Yang Huang, Qing Xiao, Feargal Brennan

Faculty of Engineering, University of Strathclyde, Glasgow G4 0LZ, UK

University of Strathclyde, Glasgow, UK

Email: farhad.abad@strath.ac.uk

Abstract

The study introduces the novel idea of using structured natural rubber, resembling Auxetic patterns, in Oscillating Water Column (OWC) Wave Energy Converters (WECs). These membranes exhibit a non-linear stiffness that increases with higher pressure in the air chamber and harsh environmental conditions. They also exhibit differing behaviours depending on the deformation mode. To accurately capture their responses, bulge testing is employed, simulating the deformation mode within OWC devices. This novel idea is combined with a sophisticated characterisation technique to find homogenised hyperelastic models. The study aims to enhance OWC efficiency and reliability by identifying optimised membrane geometries and properties. Moving forward, model refinement and further experiments will validate findings and drive progress in this field. Our future work will use the obtained hyperelastic models in fluid-structure interaction simulations of structured membranes in OWCs.

Background

- The Oscillating Water Column (OWC) is a type of Wave Energy Converter (WEC) renowned for its simplicity and reliability.

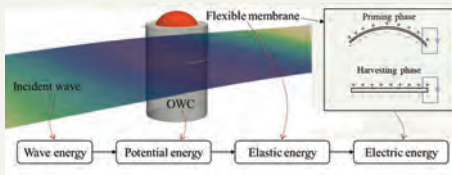


FIGURE 1: Schematic diagram of energy conversion in the novel flexible OWC.

- It utilises an air chamber that transforms wave motion into air pressure, driving a power take-off (PTO) system to generate electricity.
- In this design, elastomers are used at the top, while dielectric elastomer generators serve as the PTO mechanism, eliminating the need for traditional turbines.

Experimental Configuration and Measurement Tools

Experimental Setup Overview:

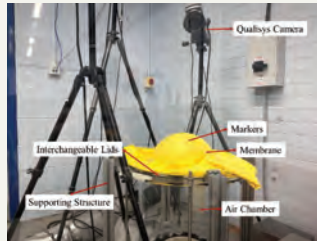


FIGURE 3: The experimental setup

Figure 3 shows the setup prepared for the bulge test.

- An acrylic cylinder is securely positioned as an air chamber.
- Elastomer membrane securely affixed to prevent leaks.
- The air pump applies consistent pressure.
- Qualisys motion capture system measures elastomer deformation using infrared light and markers.
- Three high-resolution cameras (Qualisys Oqus 300+) aid in measurement.
- A pressure transducer measures the pressure inside the air chamber.

Sample Configuration:

- The first sample (S1): Single layer of latex (natural rubber)**
 - 24 cm diameter, 0.18 mm thickness.
 - Ideal for observing structured membrane stiffness effects.
- The second sample (S2): Multi-layered configuration**
 - Latex layer with 1 mm thick structured membrane layer.
 - Enables analysis of their interaction and combined impact on stiffness.

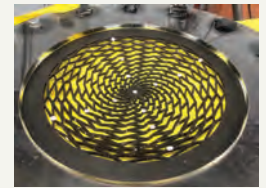


FIGURE 4: S2 Configuration

Methodology

Figure 2 illustrates the steps outlined in this process:

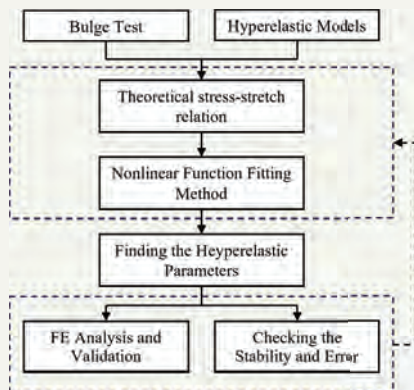


FIGURE 2: Overview of the methodology in this work.

- Pressure and deformation data will be converted into stress and stretch results.
- These results will be fitted to various hyperelastic models.
- Selected hyperelastic models will be used in numerical simulations of the bulge test.
- Suitable models are chosen based on stability conditions, error analysis, and Abaqus validation.

Numerical Results and Discussions

Figure 5 compares the stress-stretch curve between experimental results and fitted models for the second sample.

- Employed MATLAB code to fit stress-stretch data to various hyperelastic models [1].

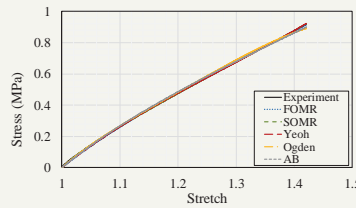


FIGURE 5: Comparison of stress-stretch curves for the second sample

Table 1: Hyperelastic parameters from diverse models for the samples are presented.

Model	Parameters	Material	
		S1	S2
FOMR	C_{10} (MPa)	0.3280	0.2271
	C_{01} (MPa)	-0.0701	0.0155
SOMR	C_{10} (MPa)	1.4956	0.6762
	C_{01} (MPa)	-1.0796	-0.3866
	C_{20} (MPa)	0.7345	0.5086
	C_{11} (MPa)	-0.3616	-0.3740
	C_{02} (MPa)	0.0798	0.0960
Ogden (N=3)	μ_1 (MPa)	0.5758	0.0071
	α_1	-4.6303	-0.249
	μ_2 (MPa)	-0.6756	17.088
	α_2	-4.6021	7.1269
	μ_3 (MPa)	0.3082	-16.534
Yeoh	α_1	8.7376	7.210
	C_{10} (MPa)	0.2689	0.2491
	C_{20} (MPa)	-0.0546	-0.0013
	C_{30} (MPa)	0.0103	0.0029

Figure 6 compares the pressure-displacement curves of both samples:

- YELLOW AREA:**
 - Low-pressure → Similar deformation levels.
- GREEN AREA:**
 - High-pressure → The second sample's nonlinear effect.

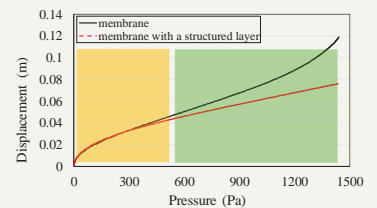


FIGURE 6: The displacement-pressure curve of samples

Conclusions:

- Characterised performance of structured membranes in OWCs using diverse hyperelastic models.
- Bulge test revealed nonlinear effects, indicating increased stiffness under higher pressure.
- Findings enhance understanding and future potential in wave energy conversion.

Reference:

- Abad, Farhad, et al. "Experimental and computational analysis of elastomer membranes used in oscillating water column WECs." *Renewable Energy* (2024): 120422.

Hinged very large floating structures for wave energy conversion and wind turbine foundation

Abel Arredondo-Galeana^a, Maurizio Collu^a, Feargal Brennan^a

^a Department of Naval Architecture, Ocean and Marine Engineering, University of Strathclyde

In this work, we explore the concept of a hinged very large floating structure (VLFS) to support multiple wind turbines and extract wave energy through hinge motion. Wave energy extraction can complement wind energy generation at times when the turbine needs to be shut down due to low or high winds. With such hybrid platform, a stable power supply could be achieved for applications that require constant power, such as electrolyzers for offshore hydrogen generation. Furthermore, multiple wind turbines in a single floating platform can represent a cost reduction in offshore installations and a reduced environmental impact through a reduction in mooring lines.

A hydroelastic numerical model is implemented to predict the motion of the platform and the hinge through a discrete-beam-module approach [1]. The turbine mass and thrust will be coupled initially in the frequency domain to the hydrodynamic model, and in a subsequent step in the time domain. Initially, we study the case of a single turbine and a hinged VLFS, depicted in Figure 1a. The pitch angle θ of the hinge can be computed through the hydrodynamic model, and therefore the angular velocity ($\dot{\theta}$) and acceleration ($\ddot{\theta}$). For rotary systems that extract energy [2], the equation of motion is

$$\tau_{hydro} - \tau_{PTO} = I\ddot{\theta},$$

where τ_{hydro} is the hydrodynamic torque on the hinge, τ_{PTO} is the power take-off torque and I is the moment of inertia (Figure 1b). Then, the power captured by the hinge is

$$P = \tau_{pto}\dot{\theta}.$$

The complementarity of wind and wave energy resources will be explored through the correlation of the wind power and the wave energy extracted. Metocean data from the ERA 5 data base from the ESOX tool will be used. Preliminary results for the upstream hinge angle of the platform are shown in Figure 1b. Results indicate that there is a resonant frequency and that pitch angle of the hinge grows with wave height.

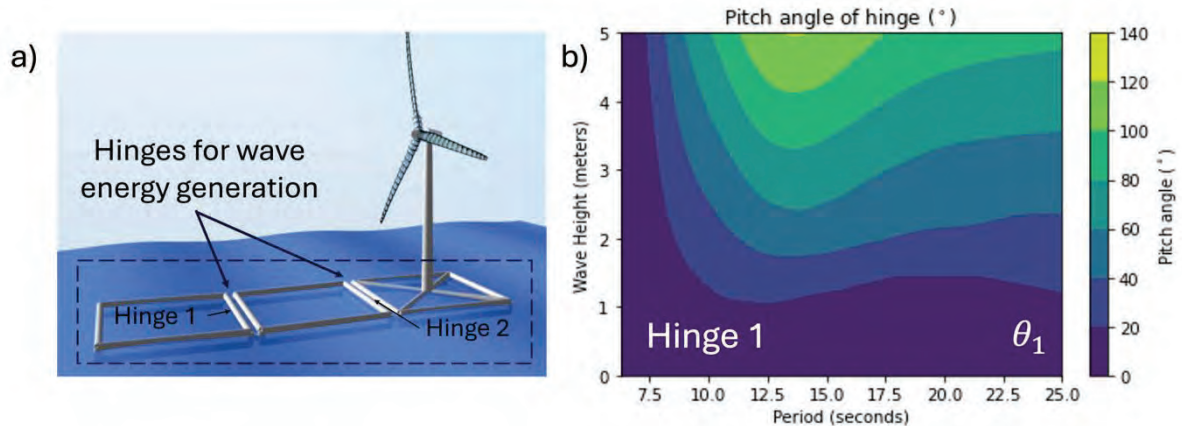


Figure 1 a) Hinged very large floating structure (VLFS) with 5MW NREL wind turbine and b) pitch angle for the first hinge as a function of period and wave height.

[1] Arredondo-Galeana, A., Dai, S., Chen, Y., Zhang, X., & Brennan, F. (2023). Understanding the force motion trade off of rigid and hinged floating platforms for marine renewables. *Proceedings of the European Wave and Tidal Energy Conference*, 15, 1-10.

[2] Arredondo-Galeana, A., Ermakov, A., Shi, W., Ringwood, J. V., & Brennan, F. (2024). Optimal control of wave cycloidal rotors with passively morphing foils: an analytical and numerical study. *Marine Structures*, 95, Article 103597.

Hinged very large floating structures for wave energy conversion and wind turbine foundation

Dr Abel Arredondo-Galeana^a, Professor Maurizio Collu^a, Professor Feargal Brennan^a
^a Department of Naval Architecture, Ocean & Marine Engineering, University of Strathclyde

Background

In this work, we explore the concept of a hinged very large floating structure (VLFS) to support multiple wind turbines and extract wave energy through hinge motion. Wave energy extraction can complement wind energy generation at times when the turbine needs to be shut down due to low or high winds. With such hybrid platform, a stable power supply could be achieved for applications that require constant power, such as electrolyzers for offshore hydrogen generation. Furthermore, multiple wind turbines in a single floating platform can represent a cost reduction in offshore installations and a reduced environmental impact through a reduction in mooring lines.

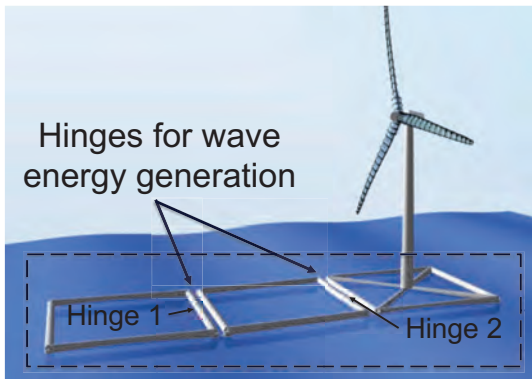


Figure 1– Hinged very large floating structure (VLFS) with 5MW NREL wind turbine

We study the case of a single turbine and a hinged VLFS (Figure 1). The pitch angle θ of the hinge can be computed through the hydrodynamic model, and therefore the angular velocity ($\dot{\theta}$) and acceleration ($\ddot{\theta}$). For systems that rotate and extract energy [2], the equation of motion is

$$\tau_{hydro} - \tau_{PTO} = I\ddot{\theta},$$

where τ_{hydro} is the hydrodynamic torque on the hinge, τ_{PTO} is the power take-off torque and I is the moment of inertia (Figure 2). Then, the power captured by the hinge is

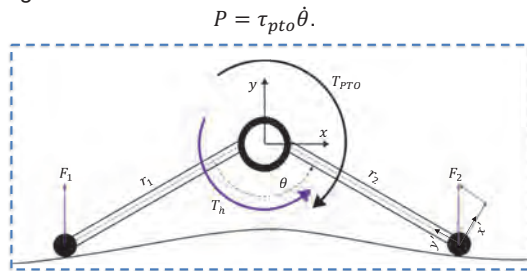


Figure 2– Hinge dynamic model details

Wind wave correlation

The complementarity of wind and wave energy extraction through the hinged VLFS is explored first through the correlation of the wind and wave energy resources. Secondly, the correlation of the wind power and the wave energy extracted will be assessed. As an example, Figure 3 shows Meteocean data from the ERA 5 data base from the ESOX tool for a location with low correlation of the coast of Spain, Villagro Sisagras.

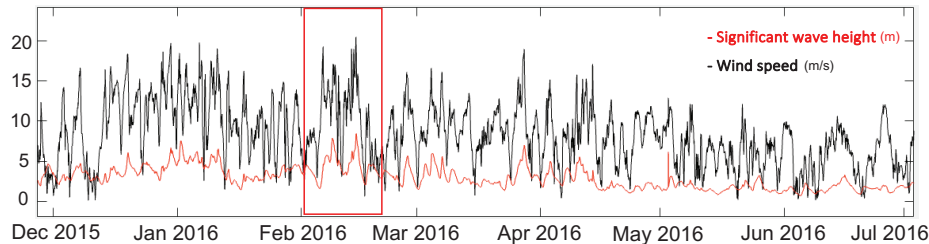


Figure 3– Wind and wave meteocean data from Villagro Sisagras, coast of Spain showing low correlation areas

Hydroelastic model of VLFS

The hydroelastic numerical model predicts the motion of the platform and the hinge through a discrete-beam-module approach (Figure 4). The model is described in detail in [1]. The turbine mass and thrust will be coupled initially in the frequency domain to the hydrodynamic model, and in a subsequent step in the time domain.

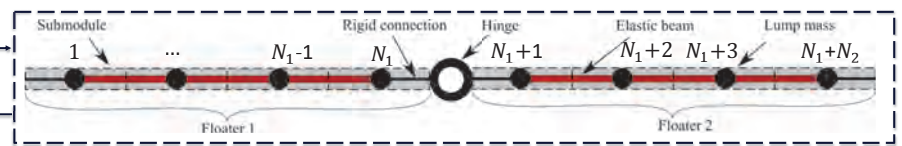


Figure 4– Hydroelastic model for the hinged VLFS (showing one hinge only)

Results

The amplitude of the heaving motion response (Δz) of the hinged VLFS (without turbine) is illustrated in Figure 5a for a regular wave of similar wavelength to the length of the VLFS ($\lambda/L \approx 1$). The numerical prediction (solid line) is compared to experimental data (markers) measured at different wave heights in the Kelvin Hydrodynamics Laboratory at the University of Strathclyde. Results are normalised with wave height. Figure 5a shows Δz along different stations of the VLFS along the normalised horizontal axis (x/l). Using the numerical and experimental results of Δz , Figure 4b shows the computed pitch angle for one of the hinges shown in Figure 1. Preliminary analysis of Figure 4b shows that there is a resonant frequency and that pitch angle grows with wave height.

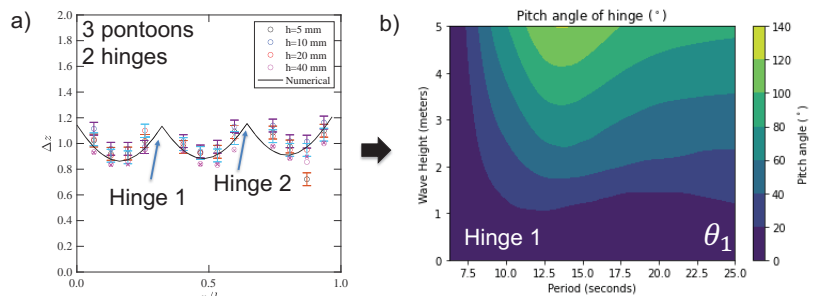


Figure 5– a) Heaving amplitude of hinged VLFS for $\lambda/L \approx 1$, and b) pitch angle for the first hinge as a function of period and wave height.

References

- Arredondo-Galeana, A., Dai, S., Chen, Y., Zhang, X., & Brennan, F. (2023). Understanding the force motion trade off of rigid and hinged floating platforms for marine renewables. Proceedings of the European Wave and Tidal Energy Conference, 15, 1-10. <https://doi.org/10.36688/ewtec-2023-389>
- Arredondo-Galeana, A., Ermakov, A., Shi, W., Ringwood, J. V., & Brennan, F. (2024). Optimal control of wave cycloidal rotors with passively morphing foils: an analytical and numerical study. Marine Structures, 95, Article 103597. Advance online publication. <https://doi.org/10.1016/j.marstruc.2024.103597>
- Arredondo-Galeana, A., Chen, Y., Dai, S., Zhang, X., Brennan, F. (2024). "Motion and load performance of rigid and hinged very large floating platforms" (Journal article in preparation).

Soil Reaction Curves for the Response of Monopile Tip in Clay

Abigail H. Bateman¹ and Cam Walker

Department of Civil Engineering, University of Bristol, Bristol, UK

¹a.bateman@bristol.ac.uk

Traditional “p-y” models, commonly employed to obtain the response of laterally loaded piles, tend to overpredict the displacement response of the squat monopile foundations often used for offshore wind turbines. To improve this, distributed shaft moment-rotation curves as well as load-displacement and moment-rotation curves at the pile base have been proposed. Combined, these curves can make up 10-25% of the overall pile resistance [1]; but are the subject of far less published research than the commonly employed “p-y” curves. Available solutions for the base curves are limited to those using basic similarity assumptions [2] or those fitted to complex numerical/empirical results developed for specific soil/pile configurations [3].

In this work, expressions for simplified shear base curves are developed using a cone model solution combined with a power-law soil constitutive model [4]. This is expressed in closed-form and shows a very close match to available similarity solutions. The results can be used in conjunction with p-y curves to obtain the full displacement response of monopile foundations without the need for a time-consuming 3D numerical analysis or expensive field testing. This is particularly useful in the early stages of design to offer a non-linear design method before advanced numerical modelling is conducted.

- [1] Murphy, G., Igoe, D., Doherty, P., Gavin, K., 2018. 3D FEM approach for laterally loaded monopile design. *Computers and Geotechnics* 100, 76–83. <https://doi.org/10/gds5q4>.
- [2] Zhang, Y., Andersen, K.H., 2019. Soil reaction curves for monopiles in clay. *Marine Structures* 65, 94–113. <https://doi.org/10.1016/j.marstruc.2018.12.009>.
- [3] Byrne, B.W., Houlsby, G.T., Burd, H.J., Gavin, K.G., Igoe, D.J.P., Jardine, R.J., Martin, C.M., McAdam, R.A., Potts, D.M., Taborda, D.M.G., Zdravković, L., 2020. PISA design model for monopiles for offshore wind turbines: application to a stiff glacial clay till. *Géotechnique* 70, 1030–1047. <https://doi.org/10.1680/jgeot.18.P.255>
- [4] Walker, C., 2024. Simplified prediction methods for non-linear offshore monopile base reaction curves in clay. Undergraduate Research Report No. 2324RP087. Civil Engineering Programme, School of Civil, Aerospace and Design Engineering, University of Bristol, Bristol, U.K.

Soil Reaction Curves for the Response of Monopile Tip in Clay

1 Response of Monopiles

Monopiles, the primary foundation choice for offshore wind turbines, face horizontal/moment loads at the pile head from wind/wave loading.

Understanding monopile response aids **efficient design**. A simplified method discretises the pile into slices and defines **soil reaction curves**.

For the pile shaft, "**p-y**" curves and "**m-θ**" curves describe the distributed horizontal force-displacement and moment-rotation response.

For the pile base:

- "**H_b-y_b**" curves describe the horizontal force-displacement response at the pile base.
- "**M_b-θ_b**" curves describe the moment-rotation response at the pile base.

2 What is the problem?

Solutions for the pile base are **limited** to fitting through site-specific FEA (Byrne et al. 2020) or similarity approaches (Zhang & Anderson 2019).

This simplified solution enables **non-linear closed-form base reaction curves** that are not specific to soil conditions – advantageous early in the design process.

3 Proposed solution: Cone Model

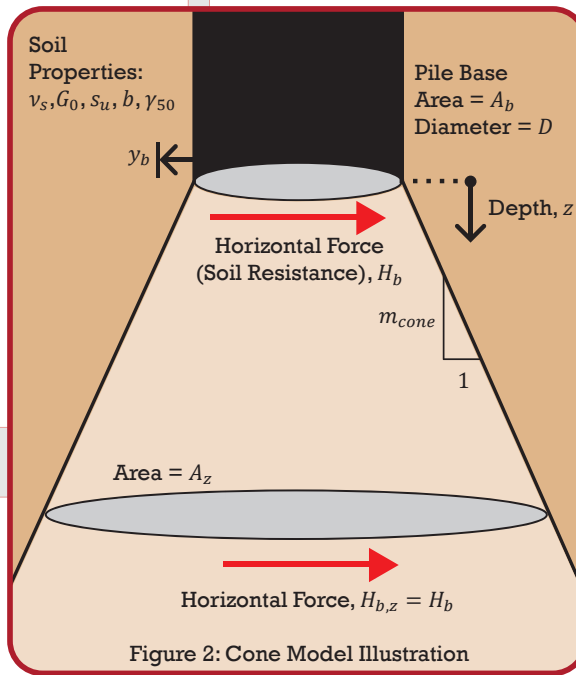


Figure 2: Cone Model Illustration

"**H_b-y_b**" curves are derived from a **cone model** (Fig. 2) to depict the vertical attenuation of soil stresses.

The stresses in the soil are related to strains using a **non-linear** soil model, e.g. a power-law:

$$\tau = \frac{s_u}{2} \left(\frac{\gamma}{\gamma_{50}} \right)^b$$

where τ, γ are the shear stress and strain in the soil.

Integrating the resultant soil strain with respect to depth gives the horizontal displacement, y_b , as a function of the applied force:

$$y_b = \int_0^\infty \varepsilon(z, H_b) dz$$

where ε is the normal strain within the soil.

4 Results and Conclusions

Novel "H_b-y_b" curves are derived in closed-form (Fig. 3) using simplified non-linear soil models applied with a cone model. Similar methods can be applied to find base moment-rotation solutions.

The solution is compared to a "**similarity**" result by Zhang and Anderson (2019) who suggested the x-axis of a stress-strain curve can be compressed by a factor of 0.12 to obtain a base curve.

These can be used in conjunction with available shaft soil reaction solutions to efficiently design monopiles for **offshore wind turbines**.

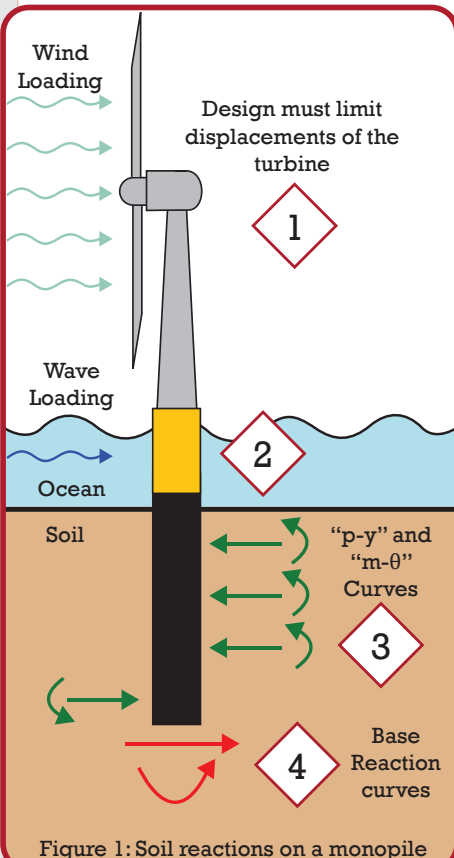


Figure 1: Soil reactions on a monopile

1

Horizontal wind and wave loading acts laterally on the wind turbine.

2

The loading is represented at the pile head by a horizontal load and a moment.

3

This can be modelled using simplified soil reaction curves along the pile shaft.

4

As well as lateral and moment soil reaction curves at the pile base.

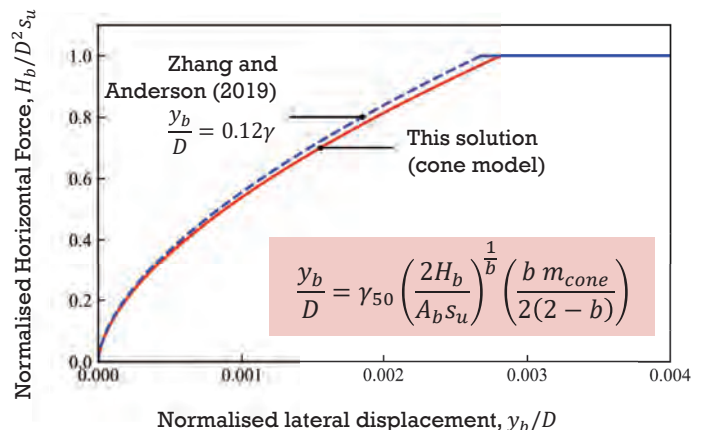


Figure 3: "**H_b-y_b**" curve derived from the Cone Model using a Power-Law

Durability of polymer composite materials for ORE applications

Jasmine Bone¹; Stefanos Giannis²; Paul Smith¹

¹University of Surrey, ²National Physical Laboratory

The durability assessment of polymer composite materials for offshore renewable energy turbine blades requires an understanding of the material degradation mechanisms that occur in these environments. There are significant challenges in ensuring the validity of accelerated ageing procedures and characterisation of degradation of these materials due to environmental exposure, for representative service lifetime predictions.

In this work, accelerated ageing methods have been used to study the degradation of carbon fibre reinforced polymer (CFRP) composite materials when exposed to various elevated temperature and humidity conditions. The effects of moisture diffusion on material properties have then been characterised using macro scale tests such as microscopy, dynamic mechanical analysis, and four-point bend flexure. While these macro scale tests indicate degradation at the fibre-matrix interface is significant in the reduction of mechanical properties such as strength and modulus, micromechanical testing is required to assess this interfacial degradation more fully. Therefore, nanoindentation testing through the thickness of a composite cross section has been employed as a localised assessment of hardness and modulus at the microscale. This offers a more nuanced understanding of the mechanical properties at the microstructural level and will be developed for better modelling of material changes due to diffusion.

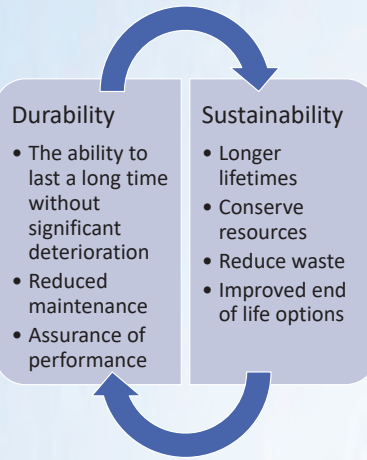
The development of research activity on durability assessment of polymeric materials underpins sustainability, resource efficiency, and both materials selection in design and end of life considerations for numerous applications and industrial sectors. It is therefore essential to improve methods for ageing assessment and lifetime predictions.

Jasmine Bone¹; Stefanos Giannis²; Paul Smith¹
¹University of Surrey, ²National Physical Laboratory

Introduction

The durability assessment of polymer composite materials for offshore renewable energy turbine blades requires an understanding of the degradation mechanisms in these environments. There are significant challenges in ensuring the validity of accelerated ageing procedures and characterisation of degradation of these materials due to environmental exposure, for representative service lifetime predictions¹.

In this work the degradation of fibre reinforced polymer (FRP) composite materials exposed to various temperature and humidity conditions, and the changes in material properties have been correlated with the exposure to identify the state of the material degradation. This will inform end-of-life options for FRP composite structures.



Methods and Materials

A unidirectional carbon fibre epoxy composite strip has been used in this testing.

To simulate the effects of long-term exposure of polymer composite materials, specimens have been exposed to increased severity test conditions to accelerate water uptake

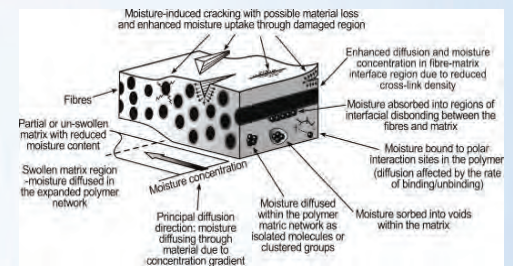


Figure 1. Diffusion of water into a composite material².

Accelerated ageing

FRP samples were exposed in a water bath at 23, 40 or 60°C, and in pressure vessels filled with deionised water at 300 bar and 60°C.

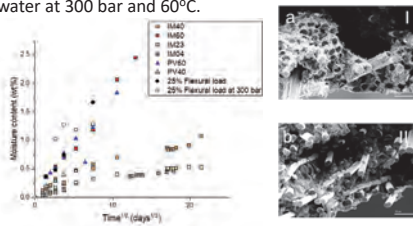


Figure 2. Moisture uptake in CFRP composite material³ (above), and fracture surface of CFRP specimens aged at 0, 7 and 56 days³ (right)

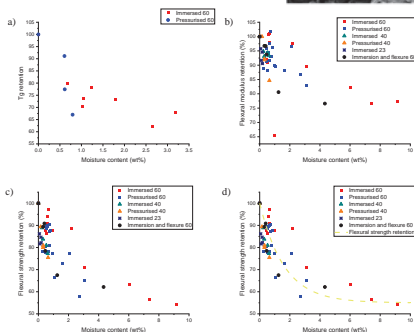


Figure 3. Decrease in flexural strength, modulus and glass transition temperature with moisture uptake of CFRP³.

Results show a reduction in material properties due to moisture ingress.

Plasticisation of the polymer matrix reduces the glass transition temperature.

Interfacial degradation reduces load transfer and therefore reduces strength and stiffness.

Characterisation at the interface

It has been shown that moisture absorption in FRPs reduces mechanical properties, likely due to interfacial degradation^{3,4}.

Nanoindentation can be a useful tool to measure through thickness micromechanical properties⁵.

Testing using this method has shown differences in load displacement curves. Figure 4 shows this distinction in matrix, interphase, and fibre regions.

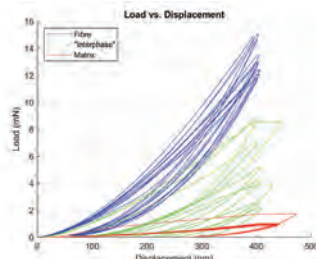


Figure 4. Load displacement curve for indents in an unaged CFRP cross section. Indents were only left in resin areas of the cross section, not on the fibres due to elastic response of the polymer.

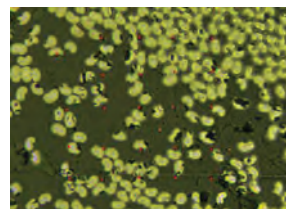


Figure 5. Cross section of CFRP composite showing location of nanoindentation

A difference in bulk matrix hardness and modulus at the edge of specimen compared to centre of specimen – shows moisture ingress through the thickness of the sample.

Discussion

Use of elevated temperature accelerates the rate of moisture uptake in polymeric materials. The addition of a mechanical load during exposure can also increase moisture uptake due to damage. However, exposure in water at elevated pressure does not significantly affect moisture ingress.

While the reduction in material properties with moisture ingress is clear, and nanoindentation testing shows initial results can differentiate the composite regions, further testing is required on samples exposed in different conditions to relate micromechanical property changes to macro scale test results.

Additional image analysis will enable quantification of the indent distance from the fibres, and better understanding of the interfacial degradation with measurement of the hardness and stiffness.



Conclusions and next steps

Accelerated ageing can be used to simulate offshore exposure, and various characterisation techniques can be used to correlate moisture uptake with material property changes. However, to better model this for lifetime prediction, interfacial degradation needs to be better studied. Future work will involve development of composite materials with different fibre sizings to test interfacial strength. Additionally, this work will be developed on an additively manufactured carbon fibre composite material; both for understanding material ageing and interfacial degradation.

Contact

Dr Jasmine Bone
University of Surrey
Email: jasmine.bone@surrey.ac.uk
Website: <https://www.surrey.ac.uk/people/jasmine-bone>
<https://www.linkedin.com/in/jasmine-bone-26861032/>

References

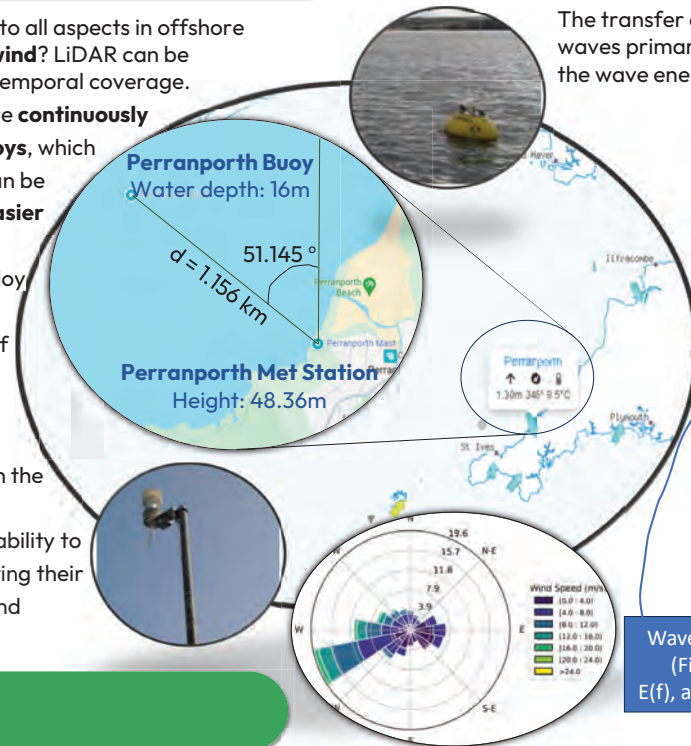
- A. S. Maxwell and W. R. Broughton, Survey of long-term durability testing of composites, adhesives and polymers, NPL Report, MAT85, November 2017
- D. A. Bond and P. A. Smith, "Modeling the transport of low-molecular-weight penetrants within polymer matrix composites," *Appl. Mech. Rev.*, vol. 59, no. 1-6, pp. 249-267, 2006, doi: 10.1115/1.2202873.
- J. E. Bone, On the Effect of Accelerated Ageing and Moisture Absorption in Polymer Composites, Doctoral Thesis, University of Surrey, 2021
- J. E. Bone, G. D. Sims, A. S. Maxwell, et al. On the relationship between moisture uptake and mechanical property changes in a carbon fibre/epoxy composite. *Journal of Composite Materials*. 2022;56(14):2189-2199. doi:10.1177/00219983221091465
- H. Pérez-Martin, P. Mackenzie, A. Baidak, C. M. Ó Brádaigh, D. Roy, Microstructural and micromechanical property characterisation of CF/PEKK composites using nanoindentation, *Materials & Design*, Volume 234, 2023,

Estimating Wind Using Wave Buoy Measurement: A case study in the Celtic Sea

Abstract: In offshore wind energy development, precise wind data acquisition is pivotal for site assessment, operation, and safety. Traditional methods like LiDAR, though accurate, are costly, while satellite data often lacks the required resolution. This study presents an alternative approach using wave buoys, which are cost-effective and easily deployable in large numbers due to their compact size. Focusing on a case study in the Celtic Sea, the research investigates the feasibility of estimating wind conditions based on wave buoy measurements, particularly looking at the high-frequency portion of the wave spectrum known as wind-sea. The analysis employs measured wave and wind data from a site that presents both types of measurements, albeit at slightly different locations. The study finds that wave buoy data, through tailored modelling, can indeed serve as a reliable source for estimating wind speed and direction. The derived U10 wind parameter shows promising results, outperforming interpolated data from ERA5, especially in calmer conditions. When compared with ERA5, the modelled wind speeds are more accurate, with an RMSE of 2.7 m/s, and wind direction estimates are within an RMSE of 26 degrees, indicating substantial potential for wave buoys in wind energy assessments.

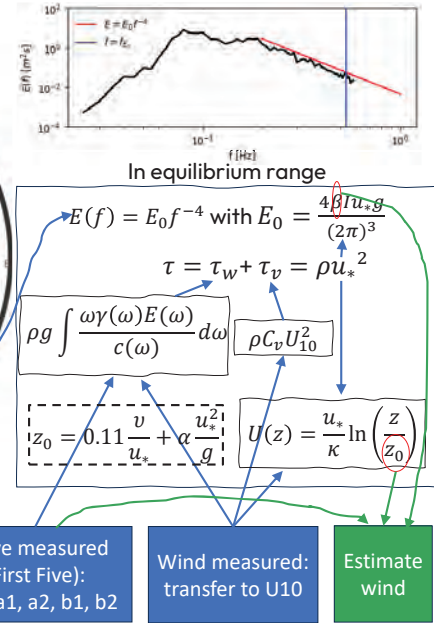
1 Purpose

- Accurate wind data can be beneficial to all aspects in offshore wind. How do we **measure offshore wind**? LiDAR can be expensive; Satellites lack spatial and temporal coverage.
- Coastal marine weather conditions are **continuously** monitored by wave Buoys. **Wave buoys**, which measure waves only and not wind, can be more compact, which makes them **easier to deploy**, relatively low cost, and therefore, much better suited to deploy in larger numbers.
- This study evaluates the practicality of wave buoys for offshore wind measurement as a **cost-effective** alternative to LiDAR and satellites. The measured data from a site within the Celtic Sea water area is explored.
- The goal is to assess wave buoys' capability to provide sufficient wind data, supporting their deployment for efficient offshore wind resource assessment.

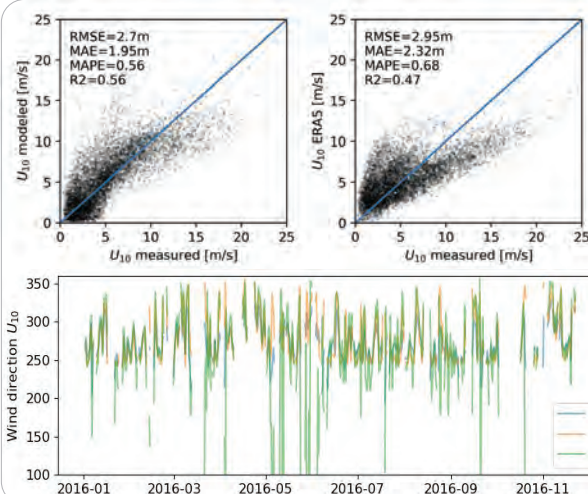
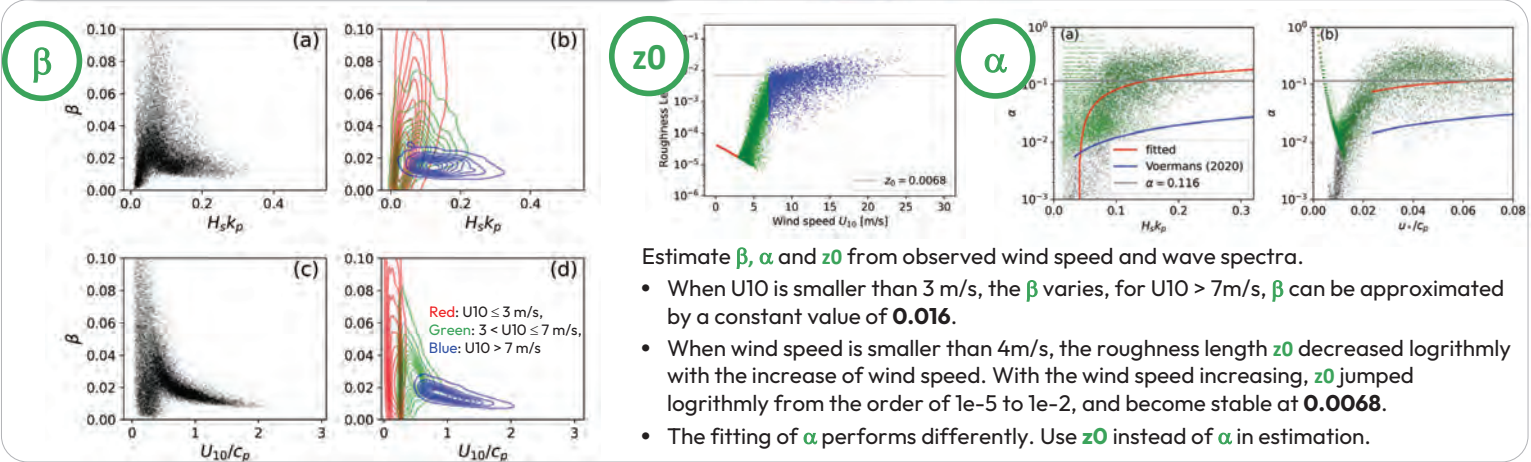


2 Methods

The transfer of momentum from the wind to surface waves primarily occurs at the high-frequency end of the wave energy spectrum $E(f)$, i.e. spectral tail.



3 Results



Use the parameters set above and wave spectra to estimate wind based on modelled relationship.

- The modelled U_{10} performs better than ERA5 interpolated values.
- When wind is calm, modelled data tends to be scattered. When wind is severer, ERA5 tends to underestimate.
- Strong winds are intuitively concentrated in the direction between 240 and 360 and have better performance.
- Other directions may be disturbed by land. When filtering directions, the modelled direction performs well (RMSE = 26 degree)

4 Conclusions

- The modelled U_{10} outperforms the ERA5 interpolated wind data in terms of wind speed and direction, especially when wind is stronger.
- Wind estimates based on wave measurements have an RMSE of 2.7 m/s for wind speed and 26 degrees for wind direction in the dominant directions.
- The results show substantial potential for using cost-effective wave buoys in wind energy assessments and predictions.

Reference: [1] Voermans, J. J., Smit, P. B., Janssen, T. T., & Babanin, A. V. (2020). Estimating wind speed and direction using wave spectra. *Journal of Geophysical Research: Oceans*, 125(2), e2019JC015717.

[2] Shimura, T., Mori, N., Baba, Y., & Miyashita, T. (2022). Ocean surface wind estimation from waves based on small GPS buoy observations in a bay and the open ocean. *Journal of Geophysical Research: Oceans*, 127(9), e2022JC018786.

Acknowledgements: This work was funded by University of Plymouth and the EPSRC-funded SuperGen ORE Hub

CoTide: Multi-rotor utility-scale Tidal Energy Concepts

Xiaosheng Chen and Richard Willden

Department of Engineering Science, University of Oxford, Oxford, UK, xiaosheng.chen@eng.ox.ac.uk

Tidal energy is receiving increasing attentions nowadays and is regarded as an important renewable energy source to help countries reach their net-zero targets. Among the different configurations, multi-rotor systems with utility scale turbines are attractive to the industry as cost savings can be realised by sharing the support structures. Additionally, it has been demonstrated that potential performance (C_P) uplift can be achieved by a co-planar fence of turbines in a high local blockage arrangement by both theoretical studies [1,2] as well as experimental studies [3]. The local blockage ratio is related to both the inter-turbine spacing and the turbine-to-surface & turbine-to-seabed clearance. This is often the situation where utility-scale tidal turbines are deployed in shallow water regions. Laboratory experiments and theoretical studies are only able to provide limited information on the unsteady loading variation that originates from the anisotropic flow environment. This anisotropy leads to non-uniform blockage effects and turbine-to-turbine interactions.

The EPSRC programme grant CoTide is developing and demonstrating holistic integrated co-design processes for tidal energy devices. This includes developing better understanding of the design drivers under the hostile marine environments: waves, turbulence, motions, shear and corrosive conditions. In the presented study, utility scaled-up versions of the benchmark tidal turbine [4] are proposed and investigated under representative operation conditions. Simulations using Reynolds-Averaged Navier Stokes (RANS) and Large Eddy Simulation (LES) with embedded actuator line (AL) models are conducted on single rotors with uniform blockage, as well as 2- and 4-rotor fence configurations in confined channels. The discrete blade representation and unsteady nature of the LES-AL model helps to identify blade local variations around the azimuth, as well as the flow interactions when the blades of the neighbouring rotors pass each other.

Results show a 7% increase in C_T and 10% in C_P as device scale increases from lab-scale to utility scale, and a further uplift of 6.7% in C_P is achieved as the fence length is extended from a 2-rotor array to a 4-rotor array. Similar integrated performance and azimuthal variations are found for counter-rotating 2-rotor array cases with rotor blades in-phase and 60° out-of-phase, as well as with different inter-turbine spacings. The non-uniform flow environment and rotor interference effects lead to changes in azimuthal phase variations of angle-of-attack, ultimately resulting in changes of phase variation in local blade loadings. Decreasing rotor spacing leads to increased azimuthal fluctuation magnitudes. In the 4-rotor array case, we observe cross fence variations including a 2% higher C_P for the inboard rotors and clear changes in azimuthal phase variations of both the angle-of-attack and blade loadings compared to the outboard turbines.

References

1. T. Nishino and R.H.J. Willden, The efficiency of an array of tidal turbines partially blocking a wide channel, *J. Fluid Mech.*, 708, 596-606, 2012.
2. T. Nishino and R.H.J. Willden, Two-scale dynamics of flow past a partial cross-stream array of tidal turbines, *J. Fluid Mech.*, 730, 220-244, 2013.
3. J. McNaughton, B. Cao, A. Nambiar, T. Davey, C.R. Vogel and R.H.J. Willden, Constructive interference effects for tidal turbine arrays, *J. Fluid Mech.*, 943, A38, 2022.
4. S.W. Tucker Harvey, X. Chen, D.T. Rowe, J. McNaughton, C.R. Vogel, K. Bhavsar, T. Allsop, J. Gilbert, H. Mullings, T. Stallard, I. Benson, A. Young and R.H.J. Willden, Tidal Turbine Benchmarking Project: Stage I – Steady Flow Experiments, *Proceedings of the 15th European Wave and Tidal Energy Conference*, 3-7 Sep, 2023, Bilbao.

CoTide: Multi-rotor utility-scale Tidal Energy Concepts

Xiaosheng Chen and Richard Willden

Department of Engineering Science, University of Oxford



UNIVERSITY OF OXFORD



Background

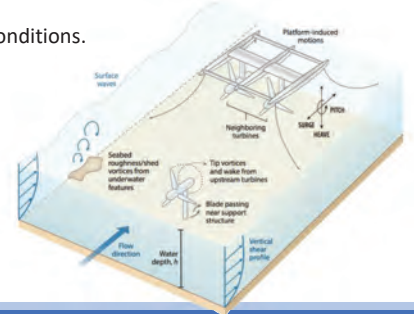
➤ **CoTide**: Co-design to Deliver Scalable Tidal Stream Energy, EPSRC programme grant, EP/X03903X/1.

- Tidal devices experience **hostile marine environments** due to waves, turbulence, motions, shear and corrosive conditions.
- Such environments lead to **complex problems** including unsteady loading, fatigue & corrosion.
- Structure design, system optimization and control are **complex with poorly understood design drivers**.

➤ Aims of CoTide:

- to develop and demonstrate **holistic integrated co-design processes** for tidal energy devices,
- leading to **better understanding of design drivers**,
- to **reduce unnecessary redundancy and improve confidence** in engineering solutions,
- leading to **reductions in both CAPEX and OPEX**.

➤ Project website: <https://cotide.ac.uk>



Rotor Concepts

➤ **Rotor hydrodynamic design**

- Initial design with scaled version of the benchmark tidal turbine¹.
- Target blockage 10% with hub velocity 2.75 m/s and inflow TI=10%.
- Concept rotor candidates:



Rotor C.ii
D=7.55 m
Fixed pitch
Rated Power ~ 0.25 MW



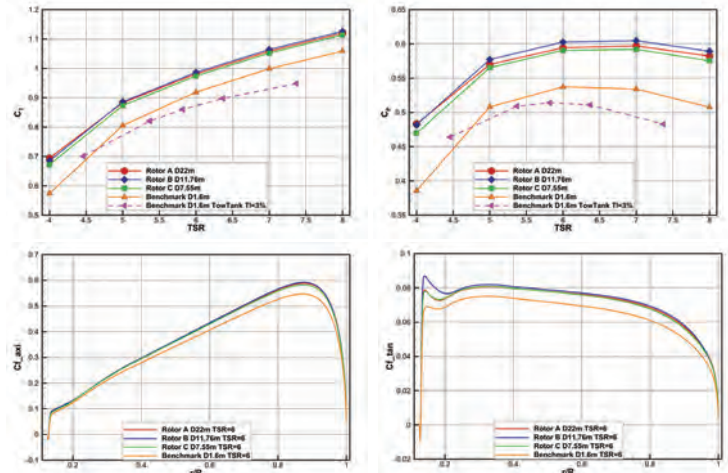
Rotor B.i/B.ii
D=11.76 m
Variable/fixed pitch
Rated Power ~ 0.6 MW



Rotor A.i
D=22 m
Variable pitch
Rated Power ~ 2 MW

➤ **Rotor performance evaluation**

- Single rotor in cylindrical domain at uniform blockage of 10%, RANS-AL simulation with 10M cells.
- Integrated performance C_T and C_P , non-dimensional axial (C_{f_axi}) and tangential (C_{f_tan}) loading distributions are examined.
- Significant changes are found from lab-scale to utility-scale: 7% increase in C_T , 10% increase in C_P . Small changes between rotors A, B and C.

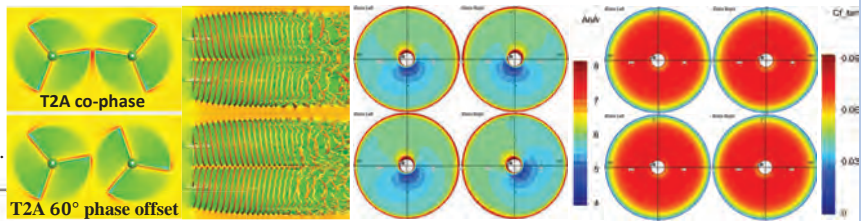
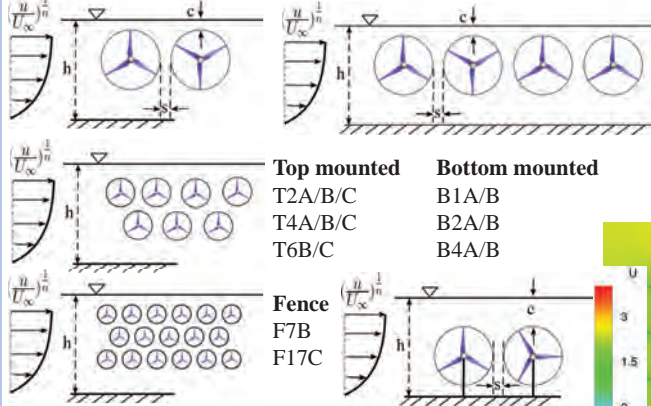


¹ S.W. Tucker Harvey et al., Tidal Turbine Benchmarking Project: Stage I – Steady Flow Experiments, Proceedings of the 15th European Wave and Tidal Energy Conference, 3-7 Sep, 2023, Bilbao.

Array Concepts

➤ **Initial concepts for array configurations**

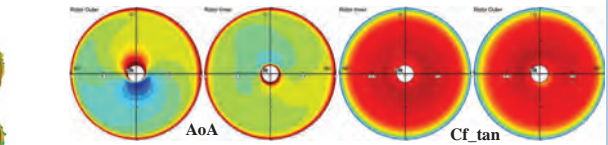
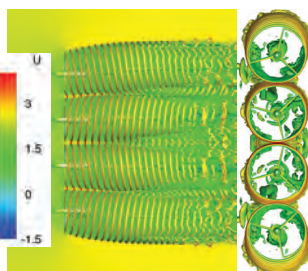
- Different rotor scales, array layouts and mounting options.
- Surface speed 3 m/s, 1/7th power law profile.
- Hub speed from 2.6 to 2.9 m/s, rated speed set to 2.75 m/s.
- By area, 2A = 7B = 17C.
- Notation: Mounting [T/B/F]-Rotor No. [1+]-Rotor Size [A/B/C].



- **T2A** with counter-rotating co-phase and 60° phase offset cases.
- Cases show similar integrated performance.
- Changes in azimuthal angle-of-attack (AoA) variation leading to phase-shifted non-dimensional tangential force distribution.

➤ **Array concepts CFD exploration**

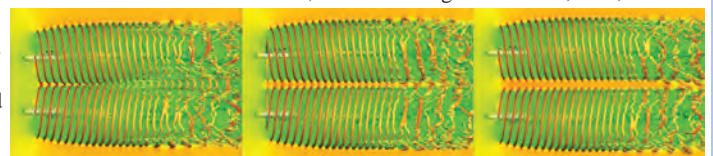
- Performance evaluated by LES-AL
- T2A, T4A simulated on 60M-cell mesh
- Uniform inflow at rated speed 2.75 m/s



- **T4A** case, array wake spreading leading to yawed approach flow to each turbine.
- C_P at TSR=6 increased to 0.602, 6.7% higher than T2A.
- C_T at TSR=6 increased to 0.9xx, 3.4% higher than T2A.
- Cross fence variations in angle-of-attack and tangential force leading to 2% higher C_P for inboard turbines.

Different s/D values for T2A, from left to right: s/D=0.05, 0.15, 0.25

- **T2A** case, with different inter-turbine spacings s/D.
- Small changes in integrated performance.
- Similar azimuthal phase variations, with increased fluctuation magnitudes for closer spacing.



Interpreting the ALPACA lateral pile load tests results: modelling accumulated displacements in chalk

Jamie Crispin¹ and Byron Byrne

Department of Engineering Science, University of Oxford, Oxford, UK

¹jamie.crispin@eng.oxford.ac.uk

Abstract:

Piles, often installed as foundations for offshore structures, are subjected to significant cyclic lateral loading due to the action of wind and waves on the structure. For piles installed in chalk, there is currently no established design method that directly incorporates the impact of these loads over the lifetime of the structure. To address the lack of guidance, this work reports the analysis of 1-way cyclic lateral load tests carried out at a chalk site as part of the ALPACA project. This is a collaboration between the University of Oxford, Imperial College London, EPSRC and industry partners (see Buckley *et al.* 2020 and Jardine *et al.* 2023 for details).

These cyclic lateral testing involved load packets including up to 2000 cycles that were applied to eight 0.51m diameter piles and one 1.22m diameter pile, with peak loads reaching 80% of the measured pile capacity. Significant accumulated displacements were observed in the direction of cyclic loading, the results of which are used to calibrate a characterisation model by LeBlanc *et al.* (2010) to capture the observed cyclic loading response. Further results are presented in McAdam *et al.* (2024). This can be used to further develop cyclic loading models used in practice.

References:

- Buckley, R.M., Jardine, R.J., Byrne, B.W., Kontoe, S., McAdam, R.A., Ahmadi-Naghadeh, R., Liu, T., Schranz, F. & Vinck, K. (2020). Pile behaviour in low-medium density chalk: preliminary results from the ALPACA project. In: *4th International Symposium on Frontiers in Offshore Geotechnics (ISFOG)*, Austin, Texas, USA, pp. 594-603.
- Jardine, R.J., Buckley, R.M., Liu, T., Byrne, B.W., Kontoe, S., McAdam, R.A., Schranz, F. & Vinck, K. (2023). Driven pile behaviour in low-medium density chalk: the ALPACA JIP outcomes. In: *Innovative Geotechnologies for Energy Transition, 9th International SUT Offshore Site Investigation and Geotechnics Conference*, London, UK, pp. 1266-1273.
- Leblanc, C., Houlsby, G.T., Byrne, B.W., (2010). Response of stiff piles in sand to long-term cyclic lateral loading. *Géotechnique*, 60, 79–90.
<https://doi.org/10.1680/geot.7.00196>
- McAdam, R.A., Buckley, R.M., Schranz, F., Byrne, B.W., Jardine, R.J., Kontoe, S., Liu, T., Vinck, K. & Crispin, J.J. (2024) Monotonic and cyclic lateral loading of piles in low to medium density chalk. *Under review*.

Interpreting the ALPACA lateral pile load tests results: modelling accumulated displacements in chalk

Jamie Crispin* & Byron Byrne
 University of Oxford, *jamie.crispin@eng.ox.ac.uk
 See Buckley et al. (2020) [1] for additional project contributors



(1) The ALPACA project

Piles, often installed as foundations for offshore structures, are subjected to significant cyclic lateral loading due to the action of wind and waves on the structure.

For piles installed in chalk, there is currently no established design method that directly incorporates the impact of these loads over the lifetime of the structure.

This is being addressed by the ALPACA project (see [1-3] for details), a collaboration between the University of Oxford, Imperial College London, EPSRC and industry partners.

This project included 1-way lateral cyclic load tests involving up to 2000 cycles that were carried out on 9 piles in chalk.

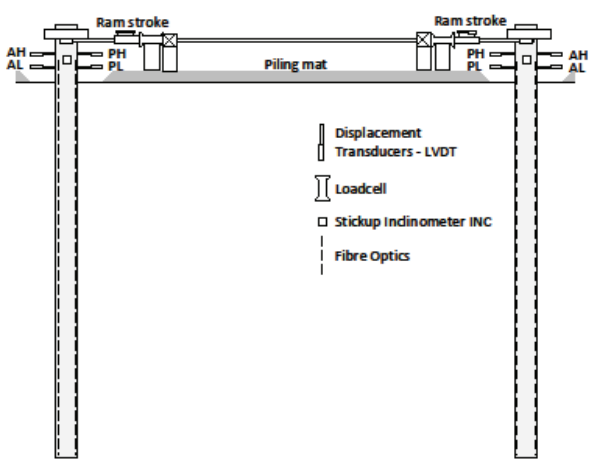


Fig. 1: ALPACA lateral 1-way test setup (reproduced from [1])

(3) Test results

The results of test 22 are shown in Fig. 3. Each pile pair was loaded against each other.

$v_{G,acc}$, the accumulated displacement can be obtained by subtracting the value on each cycle peak with the monotonic value at the peak load:

$$v_{G,acc}(N) = v_G(N) - v_{G,s}$$

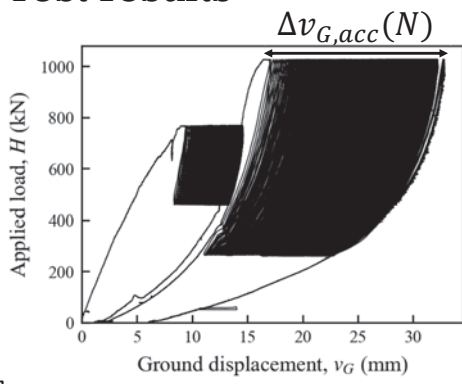


Fig. 3: Results of test 22, pile LD01

The LeBlanc et al. (2010) model has been fitted to each test result. Fig. 4 shows the fitting at $N > 100$ for pile LD01.

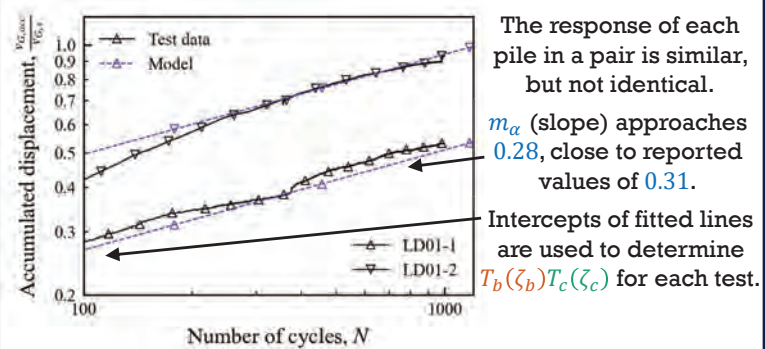


Fig. 4: Accumulated displacement for pile LD01

The response of each pile in a pair is similar, but not identical. m_α (slope) approaches 0.28, close to reported values of 0.31. Intercepts of fitted lines are used to determine $T_b(\zeta_b)T_c(\zeta_c)$ for each test.

(2) Characterisation of cyclic loading

LeBlanc et al. (2010) [4] proposed the following expression for characterising accumulated displacements during cyclic loading:

$$\frac{v_{G,acc}(N)}{v_{G,s}} = T_b(\zeta_b)T_c(\zeta_c)N^{m_\alpha} \approx 0.31$$

Annotations: $v_{G,s}$ is static v_G at H_p (peak load). $T_b(\zeta_b)$ is magnitude component. $T_c(\zeta_c)$ is asymmetry component. N^{m_α} is Number of cycles.

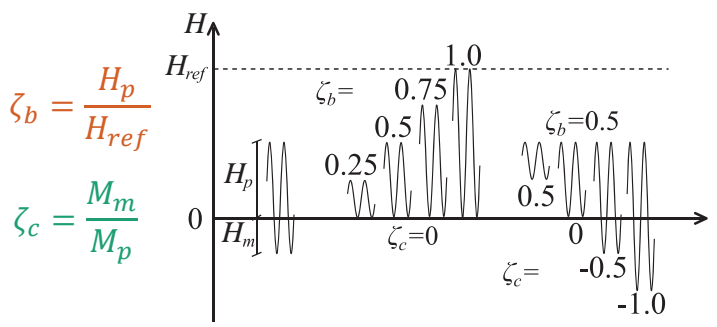


Fig. 2: Cyclic load definitions (adapted from [4])

(4) Model performance

$T_b(\zeta_b)$ and $T_c(\zeta_c)$ functions have been fit to the full dataset of pile tests. The resulting model is compared to the test data:

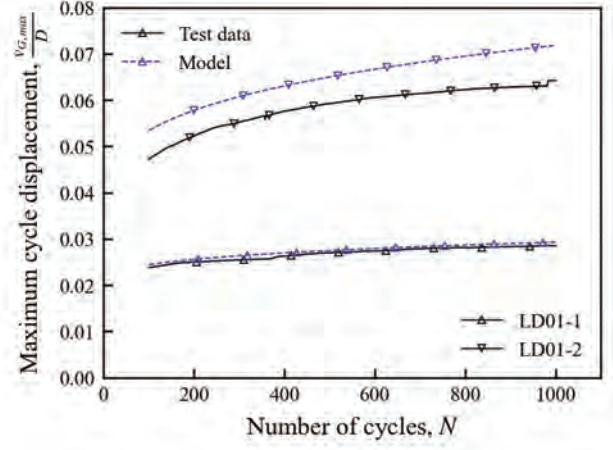


Fig. 5: Test vs. modelled accumulated displacement for pile LD01

The predicted behaviour generally falls between the results for each (identical) pile pair, indicating that the model performs well.

Further results are presented in McAdam et al (2024) [3].

References:
 [1] Buckley, R.M., Jardine, R.J., Byrne, B.W., Kontoe, S., McAdam, R.A., Ahmadi-Naghadeh, R., Liu, T., Schranz, F. & Vinck, K. (2020). Pile behaviour in low-medium density chalk: preliminary results from the ALPACA project. In: *4th International Symposium on Frontiers in Offshore Geotechnics (ISFOG)*, Austin, Texas, USA, pp. 594-603.
 [2] Jardine, R.J., Buckley, R.M., Liu, T., Byrne, B.W., Kontoe, S., McAdam, R.A., Schranz, F. & Vinck, K. (2023). Driven pile behaviour in low-medium density chalk: the ALPACA JIP outcomes. In: *Innovative Geotechnologies for Energy Transition, 9th International SUT Offshore Site Investigation and Geotechnics Conference*, London, UK, pp. 1266-1273.
 [3] McAdam, R.A., Buckley, R.M., Schranz, F., Byrne, B.W., Jardine, R.J., Kontoe, S., Liu, T., Vinck, K. & Crispin, J.J. (2024) Monotonic and cyclic lateral loading of piles in low to medium density chalk. *Under review*.
 [4] Leblanc, C., Houlsby, G.T., Byrne, B.W., (2010). Response of stiff piles in sand to long-term cyclic lateral loading. *Géotechnique*, 60, 79–90. <https://doi.org/10.1680/geot.7.00196>

Optimisation of the geometry of a top-hinged wave energy converter

Dr Emma Edwards

Career Development Fellow

University of Oxford

To reach global Net-Zero goals, renewable energy portfolios need to be sufficiently diverse. Wave energy presents an excellent opportunity to achieve this goal, since ocean waves contain enough energy to satisfy the entire global requirement for energy. However, the technology is still nascent, and wave energy conversion devices are not yet cost competitive with other renewable energy resources.

One significant challenge for wave energy is that the wave energy converter (WEC) must be able to withstand extreme forces from storms in the ocean. One type of WEC that is particularly well suited to survive these extreme events is a top-hinged WEC, which consists of a main floating WEC absorber connected to a fixed or floating structure via a hinged rigid arm. One of the benefits of this type of WEC is that the main WEC absorber can be lifted out of the sea in storms. Another challenge to wave energy is the consistent dynamic loading that devices must endure. If these forces are high, it leads to expensive support structures to withstand reaction forces.

In this work, we optimise the geometry of a top-hinged WEC to maximise power while also minimising reaction forces. This new framework for geometry optimization—including minimisation of reaction forces in the optimisation, instead of only maximisation of power—results in a promising new direction for wave energy design. We use the underlying physics of how geometry affects the wave-structure interaction to explain the resulting performance of these new WEC designs, in terms of both power and force.

In particular, we show how it is possible to significantly reduce the reaction force while only slightly reducing the extractable power. These results could lead to a new path for economic viability for wave energy, since lowering design loads while maintaining good efficiency could reduce the levelised cost of energy considerably.

LES of Wind Farms with DOFAS: Sensitivity to the SGS Model

Mina Ghobrial^a, Tim Stallard^a, David M. Schultz^{b,c}, and Pablo Ouro^{a,b}

^a School of Engineering, University of Manchester, UK

^b Centre for Crisis Studies & Mitigation, University of Manchester, UK

^c Centre for Atmospheric Science, Department of Earth & Environmental Sciences,
University of Manchester, UK

Abstract

Large-eddy simulations (LES) is a high-fidelity numerical tool used to study wakes interaction between turbines. LES can resolve the most energetic flow structures and capture the governing physics in stratified atmospheric boundary layer flows. LES adopts a sub-grid scale (SGS) model to account for the unresolved flow structures, which can be a source of uncertainty.

In this study, the inhouse LES code Digital Offshore FARM Simulator (DOFAS) is used to simulate a wind farm operating in stable atmospheric conditions with six SGS models: standard Smagorinsky, Wall-Adapting Local Eddy-Viscosity (WALE), Anisotropic Minimum-Dissipation (AMD), Turbulent Kinetic Energy (TKE), Stability Dependent Smagorinsky (SDS), and Lagrangian-Averaged Scale-Dependent Dynamic (LASDD) models. The study quantifies the impact of the SGS model on the LES by monitoring the variations in the farm wake and the farm power production between the different models.

Simulations results show dependency of LES of wind farms on the utilised SGS model, with significant variations between the models in the predicted farm performance and wake recovery. The WALE and LASDD models overpredict the low-level jet (LLJ) height, underestimate inflow speed at the turbine rotor level, and resolve a limited vertical turbulent exchange between the LLJ and wind farm compared to the other models. Regarding the accuracy of the models, SCADA data are needed to determine the model with the highest physical accuracy in such conditions.

LES of Wind Farms with DOFAS: Sensitivity to the SGS Model

Mina Ghobrial^a, Tim Stallard^a, David M. Schultz^{b,c}, and Pablo Ouro^{a,b}

^a School of Engineering, University of Manchester, UK

^b Centre for Crisis Studies & Mitigation, University of Manchester, UK

^c Centre for Atmospheric Science, Department of Earth & Environmental Sciences, University of Manchester, UK

Introduction

Large-eddy simulations (LES) is a high-fidelity numerical tool used to study wakes interaction between turbines. LES can resolve the most energetic flow structures and capture the governing physics in stratified atmospheric boundary layer flows. LES adopts a sub-grid scale (SGS) model to account for the unresolved flow structures, which can be a source of uncertainty.

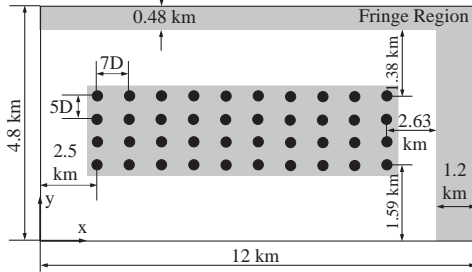
Here, LES of a wind farm in stable atmospheric conditions are performed with six SGS models: standard **Smagorinsky** [1], Wall-Adapting Local Eddy-Viscosity (**WALE**) [2], Anisotropic Minimum-Dissipation (**AMD**) [3], Turbulent Kinetic Energy (**TKE**) [4], Stability Dependent Smagorinsky (**SDS**) [5], and Lagrangian-Averaged Scale-Dependent Dynamic (**LASDD**) [6] models. The study quantifies the impact of the SGS model on the LES by monitoring the variations in the farm wake and the farm power production between the different models.



10×4 wind farm operating in a stable boundary layer.

Setup

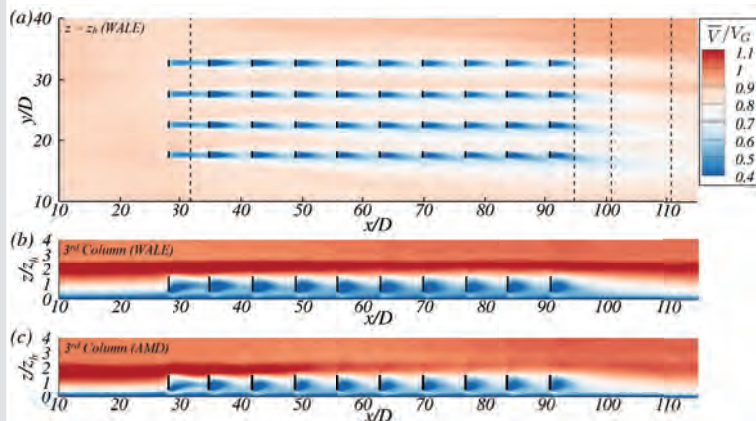
- ▶ The in-house LES code Digital Offshore FARM Simulator (DOFAS) [7] is adopted to simulate a 10×4 wind farm operating in a stable boundary layer.
- ▶ A precursor simulation according to GABLS-1 initiative with a cooling rate of 0.25 K/h is run with every SGS model to generate turbulent inflow for the wind farm simulation.
- ▶ Wind turbines are modelled with an actuator-disc method (ADM) with a diameter (D) and hub height (z_h) equal to 90 m and operating at a fixed thrust coefficient of 0.75.
- ▶ A 7.5 m grid spacing is used (i.e., there are 12 grid cells across the diameter), which provides an acceptable resolution for the ADM.



Schematic of the computational domain.

Mean velocity contours

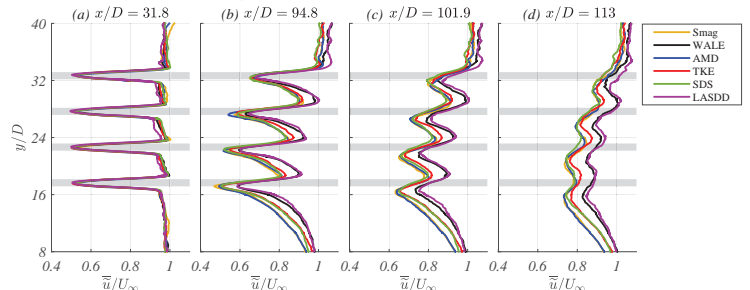
- ▶ The hub-height contours show the clockwise deflection of the wakes due to the wind veer.
- ▶ The SGS models estimate different heights of the low-level jet (LLJ). Accordingly, the models exhibit different levels of vertical entrainment from the jet to the farm.



Mean horizontal wind speed contours obtained at (a) hub height with the WALE model, (b) transverse centre of the 3rd column with the WALE model, and (c) transverse centre of the 3rd column with the AMD model.

Wind farm wake

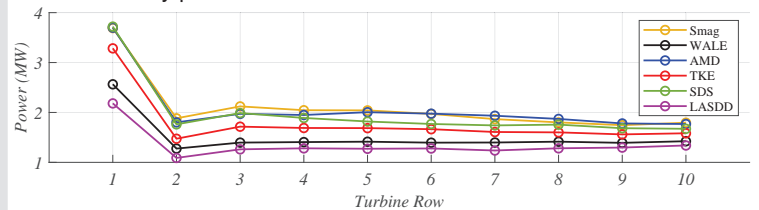
- ▶ The wake is monitored at four locations along the farm length.
- ▶ Downstream of the 1st row, all models show similar wake profiles.
- ▶ Further downstream, the WALE and LASDD models show higher wake recovery rates compared to the rest of the models.



Lateral profiles of streamwise velocity at four different locations.

Power production

- ▶ The farm power production is notably impacted by the SGS model adopted in the LES.
- ▶ The WALE and LASDD models underpredict the power production by nearly 25% than the rest of the models due to the underpredicted inflow wind speed at the turbine rotor level.
- ▶ A 50% drop in efficiency of all rows, compared to the front one, is consistently predicted in all simulations.



Conclusions

- ▶ LES of wind farms in thermally stable conditions depend on the utilised SGS model, with significant variations between the models in the predicted farm performance and wake recovery.
- ▶ The WALE and LASDD models overpredict the LLJ height, underestimate inflow speed at the turbine rotor level, and resolve a limited vertical turbulent exchange between the LLJ and wind farm.

References

- [1] Smagorinsky J 1963 *Monthly Weather Review* 91 99–164
- [2] Franck N and Ducros F 1999 *Flow Turbulence and Combustion* 62 183–200
- [3] Abkar M and Moin P 2017 *Boundary-Layer Meteorology* 165 405–419
- [4] Deardorff J W 1980 *Boundary-Layer Meteorology* 18 495–527
- [5] Stevens B, Moeng C H and Sullivan P P 2000 *IUTAM Symposium on Developments in Geophysical Turbulence* (Dordrecht: Springer Netherlands) 253–269
- [6] Stoll R and Porté-Agel F 2006 *Water Resources Research* 42 W01409
- [7] Ouro P and Nishino T 2021 *Journal of Fluids Mechanics* 925 A30

Variable amplitude fatigue testing of large scale high strength steel cast node tubular connections.

*WAMESS CDT Eng. D Researcher, John Harris
Supervisor, Professor Feargal Brennan
Faculty of Engineering, University of Strathclyde, Glasgow G4 0LZ, UK
Email: john.harris@strath.ac.uk*

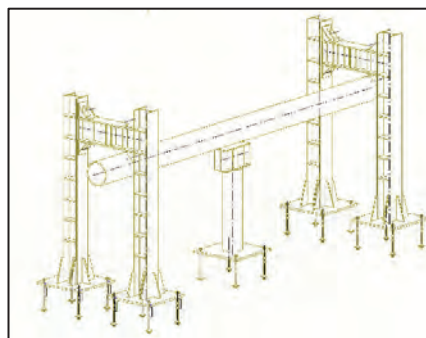
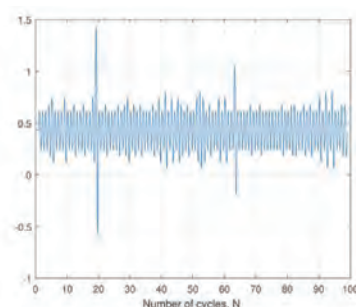
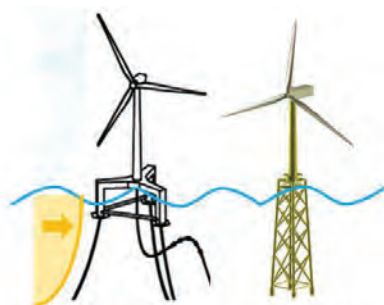
ABSTRACT

The ScotWind leasing round results of 2022 which made available seabed for commercial-scale offshore wind projects with a total capacity of 27.6GW – 17.6GW floating & 10GW fixed bottom. This coupled with the commercially viable strike price - £73/MWh fixed bottom and £176/MWh floating - announced in the latest (AR6) Contracts for Difference mean that the current Scottish wind farm project pipeline is substantial.

The 60-year length of the ScotWind seabed leases offers an opportunity to reconsider how offshore wind assets are designed - substructures could be designed for longer lifetimes. Currently the design life of offshore structures is governed by fatigue failure which happens at tubular connections where stress concentrations are high, therefore the tubular connection detail of a jacket or floating sub-structure is the focus of this research.

To increase the fatigue life of tubular connections the possibility of using high strength steel cast nodes is being explored. High strength steel brings benefits in terms of a higher yield strength which can prolong crack initiation and cast nodes can bring benefits in terms of reducing stress concentration by reducing weld complexity at the connection.

A bespoke fatigue testing rig will be designed, procured, and installed at The University of Strathclyde's heavy structures lab. The rig will be used to carry out a number of large scale fatigue tests on high strength cast steel tubular connections. Six constant amplitude load sequences and two variable amplitude load sequences - that of a typical semi submersible floater and that of a typical jacket structure - will be tested.



ScotWind

28 GW of seabed leasing rights were announced with the ScotWind results – 18GW floating and 10GW fixed bottom.

Forecast to be operational in 2030, these projects have created a **substantial UK project pipeline**.

Importantly, Scotwind offered **60 year seabed leases** which is at odds with the current design life of offshore wind assets.



Developer Opportunity

The 60 year seabed leases present an opportunity to **rethink the design of offshore assets**.

Currently many of the main components within an offshore turbines RNA will need to be **replaced at least once** during a 60 year lifecycle.

Substructures which typically represent 17% of the overall cost of an asset, could be **designed to last 60 years**.

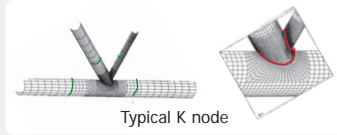


Offshore substructure design life is **governed by fatigue**.

Fatigue failure happens **at tubular connections** where weld geometries are complex.

This research aims to demonstrate an improved fatigue life by applying two existing fabrication processes and materials through **large scale testing of tubular connections**.

Cast Nodes



- Typical weld detail. SCF: 4-12

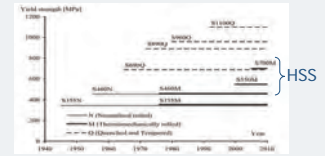
- Weld detail cast node. SCF: 1.5-4

Reduced weld complexity, reducing stress concentrations, increasing fatigue life. Existing literature shows that fatigue life of a **cast node is always better** than welded counterpart.

Other Benefits

Manufacturability. Material Reduction. Maintenance.

High Strength Steel (HSS)



Research shows that higher yield strength steel can **resist crack initiation longer**, providing the manufacturing detail is good, hence increasing fatigue life.

Other Benefits

Reduced carbon footprint. Cost reduction.

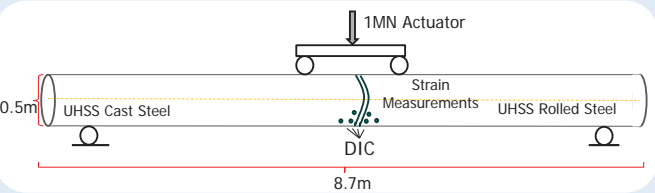
Testing Procedure

The **0.5m diameter** test specimens will be made of cast HSS and rolled HSS tubulars welded together.

Facilities at the heavy structure lab at the University of Strathclyde:

- a **200 tonne strong floor**.
- **street access** via shutter door.
- a **50 tonne gantry crane**.
- an existing **hydraulic system**.

The lab set up allows for a large scale **four point bending test**:

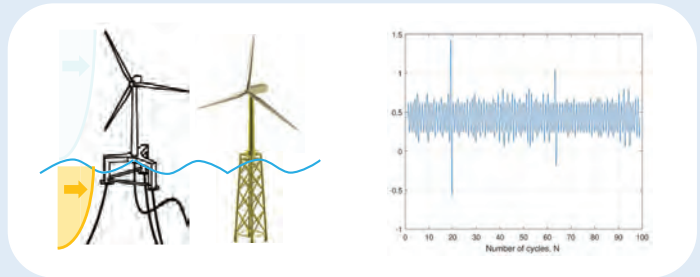


The tests will be carried out at **2Hz** requiring **12 months** to carry out **6-8 tests**.

The crack growth behaviour will be measured by **strain gauges, digital image correlation and acoustic emissions**.

Test	Loading	Mean Stress	R ratio
1	CAL	600Mpa	0.1
2	CAL	500Mpa	0.1
3	CAL	400Mpa	0.1
4	CAL	300Mpa	0.1
5	VAL	Fixed Bottom Jacket	n/a
6	VAL	Floating semi-submersible	n/a

Variable Amplitude Loading

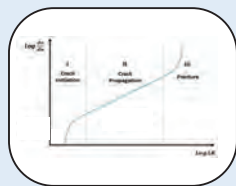


Environmental and operational dynamic loading dictate that structural components and connections experience **variable amplitudes loading sequences**. Design codes use constant amplitudes and this assumption may either be conservative or non-conservative.

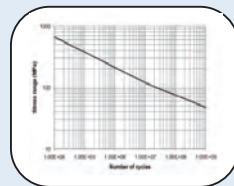
Two variable amplitude load sequences will be tested, that of a **typical semi submersible floater** and that of a **typical jacket structure**. These will be obtained by using established modelling techniques.

By imitating a VAL the aim is to develop understanding on how the variable amplitude loading impacts on **crack initiation and growth rate**.

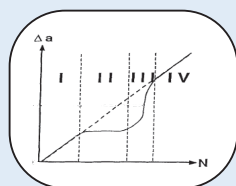
Determine if increased yield strength brings significant fatigue life benefits.



Compare fatigue life of such a connection with existing design guidance.



Understand how variable amplitude loading effects crack growth behaviour.



A sea-state-dependent power-limiting control strategy for wave energy converters

Zhijing Liao, Xiaotao Zhang, Judith Apsley, Matteo F. Iacchetti, Peter Stansby, Guang Li

Conventional control strategies for wave energy converters (WECs) maximise power capture of the WEC by amplifying its responses, but this exacerbates hardware constraint violations not generally taken into account, causing undesirable shutdown of electrical systems in adverse wave conditions. When WECs operate close to power take-off (PTO) capacity, the primary control objective is to limit peak power for hardware protection purposes, enabling longer continuous electricity generation time.

In this poster, we present a sea-state-dependent control strategy based on model predictive control to maximise the annual energy production of a WEC with a realistic PTO: in small to moderate sea states it adopts a conventional energy-maximising objective function to increase output power, while in higher sea states a speed-limiting objective function may be utilised to enable longer generating time before shutdown becomes necessary. While this control strategy applies to a wide range of WECs, here we carry out the case study on an attenuator WEC called M4, with gearbox transmission and a permanent magnet synchronous generator (PMSG) as its PTO, which is being designed for a 1/4 scale ocean test in Albany, Australia. Simulation results show that compared with a benchmark passive damping controller, a 66% increase in annual energy production can be expected at the targeted site.

A sea-state-dependent power-limiting control strategy for wave energy converters

Zhijing Liao, Xiaotao Zhang, Judith Apsley, Matteo F. Iacchetti, Peter Stansby, Guang Li

The University of Manchester, Manchester, M13 9PL, UK.

Contact: zhijing.liao@manchester.ac.uk

Abstract [1]: Conventional control strategies for wave energy converters (WECs) maximise power capture of the WEC by amplifying its responses, which exacerbates hardware constraint violations, causing undesirable shutdown of electrical systems in adverse wave conditions. **When WECs operate close to power take-off (PTO) capacity, the primary control objective is to limit peak power for hardware protection purposes, enabling longer continuous electricity generation time.** This poster introduces a sea-state-dependent control strategy to maximise the annual energy production of a WEC: in small to moderate sea states, it adopts an energy-maximising objective function to increase output power, while in higher sea states a speed-limiting objective function is utilised to enable longer generating time before shutdown becomes necessary.

Introduction

- Studied WEC platform:
 - M4 WEC with 1-2-1 configuration.
 - 20 m long, kW scale, designed for sea trial at Albany, Australia.
- All-electric PTO:
 - Gearbox transmission (ratio 739:1).
 - PM generator (6 kW).
- Integrated hydrodynamic-electrical modelling [2].
- Pseudo-steady-state modelling of the PTO to reduce simulation computational load [3].

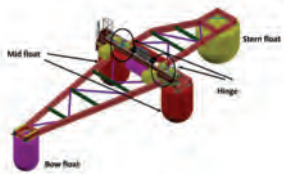


Fig. 1: The M4 1-2-1 design diagram.

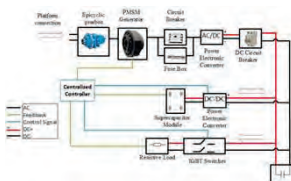


Fig. 2: The PTO design diagram.

Method

- Three stages model predictive control (MPC) scheme based on incoming sea state prediction/recognition:
 - Energy-maximising (em-MPC).
 - Speed-limiting (sl-MPC).
 - Shutting down.
- Realistic wave climate as simulation inputs.
- Hierarchical control framework.

$$\min_{U_0^N} \sum_{k=0}^N (y_k u_k + R u_k^2 + Q y_k^2)$$

$$\min_{U_0^N} \sum_{k=0}^N (R u_k^2 + Q y_k^2)$$

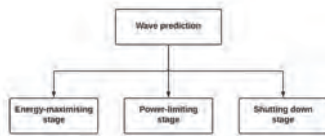


Fig. 3: Three different control stages.

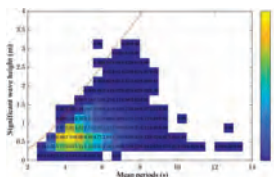


Fig. 4: Wave climate at the test site, Albany, Australia.

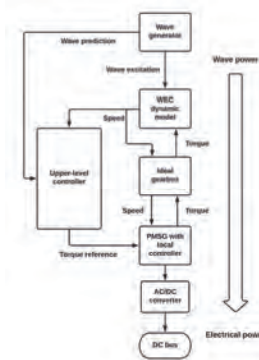


Fig. 5: The hierarchical control framework.

Results

- Power-limiting control in one extreme sea ($H_s = 1.25m$)

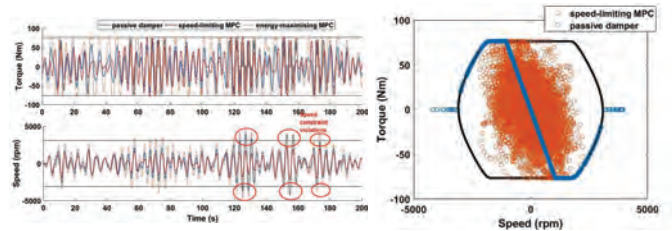


Fig. 6: Time variation of torque and speed.

Fig. 7: Time variation of torque and speed on the torque-speed curve.

- Power-limiting effect in various sea states

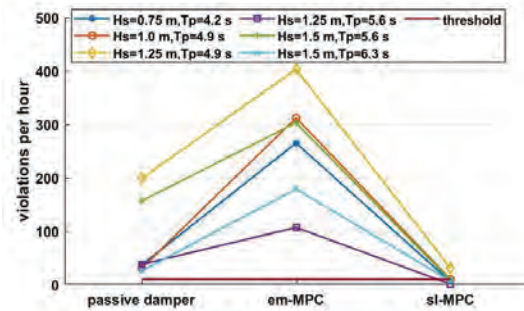


Fig. 8: Occurrence of constraint violations in the most relevant sea states with different controllers.

- Overall improvement on energy generation

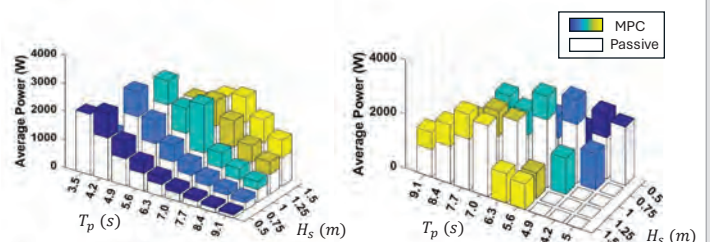


Fig. 9: Average power in each sea state with proposed MPC and passive damper, viewed from two sides.

Conclusion

- With the proposed strategy, there is a 66% improvement of electrical energy generation compared with a well-tuned passive damper.
- Only 28% with conventional em-MPC alone.
- Near PTO capacity, power-limiting control is required for WEC to protect hardware and prolong generation time.

Acknowledgement:

The authors would like to acknowledge the funding from the Engineering and Physical Sciences Research Council (EPSRC) with grant number EP/V040510/1 and EP/V040650/1. The M4 WEC was designed in the Blue Economy CRC Project Plan P.3.21.004: Seeding marine innovation in SW WA with a WEC deployment in Albany, funded by the Government of Western Australia, Blue-Economy Cooperative Research Centre, and The University of Western Australia. Fig. 1 is kindly provided by BMT, Australia.

References:

- Liao, Z., Zhang, X., Apsley, J., Iacchetti, M., Stansby, P., & Li, G. (Accepted/In press). A Sea-State-Dependent Control Strategy for Wave Energy Converters: Power Limiting in Large Wave Conditions and Energy Maximising in Moderate Wave Conditions. IEEE Transactions on Sustainable Energy. <https://doi.org/10.1109/TSTE.2024.3373121>
- Apsley, J., Zhang, X., Erazo Damian, I., Iacchetti, M., Liao, Z., Stansby, P., Li, G., Li, G., Wolgamot, H., Gaudin, C., Kurniawan, A., Zhang, X., Lin, Z., Fernando, W. U. N., Shearer, C., & Saunders, B. (2023). Integrated hydrodynamic-electrical hardware model for wave energy conversion with M4 ocean demonstrator. In 15th European Wave and Tidal Energy Conference - EWTEC Advance online publication. <https://doi.org/10.36688/ewtec-2023-500>
- Zhang, X., Apsley, J., & Iacchetti, M. (Accepted/In press). Computationally-efficient Modelling of Wave Energy Conversion Systems via Pseudo Steady-State PMSM Model. In 2023 11th International Conference on Power Electronics and ECCE Asia (ICPE 2023 - ECCE Asia)

Controlling turbine tip vortices and cavitation through local permeability

Yabin Liu^{*}, Richard H.J. Willden,[†] Paul Gary Tucker,[‡] and Ignazio Maria Viola[§].

Controlling tip vortices remains a significant challenge for wind and tidal turbines as well as for aerial and underwater vehicles. We propose and investigate the control of tip vortices through local permeability. Blade-resolved Reynolds-averaged Navier-Stokes simulation has been employed on a model-scale horizontal-axis turbine¹, following a rigorous validation and verification process. The permeable tip treatment is modelled by including a porous zone over the blade tip section, within which Darcy's law is applied. A range of tip-speed ratios for the tidal turbine, spanning from 4.52 to 7.54, has been examined.

The results have informed the determination of an optimal range of permeability, corresponding to a non-dimensional Darcy number, Da , of around 10^{-5} , that can substantially reduce the tip vortex intensity. The underlying flow physics is found to be that the permeable tip treatment can significantly enlarge the vortex viscous core radius with little change to the vortex circulation. By significantly mitigating the tip vortex intensity, the permeable tip treatment can decrease the magnitude of the minimum suction pressure coefficient at the vortex core by up to 65%, which significantly reduces the cavitation risk due to the tip vortex. The mitigation effect and optimal permeability remain consistent across tip-speed ratios ranging from 4.52 to 7.54. The spanwise extent of the permeable tip treatment is only 0.1% of the turbine diameter, and so the influence on the turbine's energy-harvesting performance is small: approximately 0.75% drop in power coefficient and 1.1% drop in thrust coefficient are observed at a tip-speed ratio of 6.03. These findings demonstrate this approach's promise to alleviate concerns about wake, cavitation and noise caused by tip vortices around wind/tidal turbines.

In summary, the revealed physics of controlling a trailing tip vortex through local tip permeability may inspire novel technologies for passive flow control through new material or structural designs. Additionally, existing investigations support the potential of local permeability in suppressing noise, which will be explored in our future simulations. We aim to develop novel blade structures to produce an equivalent permeable effect within numerical and experimental approaches in future. The underlying physics and flow control technology will broadly contribute to improving the design of turbomachinery and aerial/underwater vehicles.

^{*}School of Engineering, University of Edinburgh, Edinburgh, EH9 3BF, UK; Yabin.Liu@ed.ac.uk

[†]Department of Engineering Science, University of Oxford, Oxford, OX1 3PJ, UK.

[‡]Department of Engineering, University of Cambridge, Cambridge CB2 1PZ, UK.

[§]School of Engineering, University of Edinburgh, Edinburgh, EH9 3BF, UK.

¹Liu et al., *The 15th European Wave and Tidal Energy Conference* **15** (2023).

Background and Concept

Tip vortices cause wake, cavitation and noise concerns for wind and tidal turbines. As tidal turbines operate underwater and their blade tips experience the highest flow speeds, cavitation may occur due to low pressure inside the tip vortex at high tip speed ratios (TSRs). This can limit turbine power efficiency, leading to an upper TSR limit, and result in blade erosion, vibration, and cavitation noise due to bubble collapse. Therefore, considerable attention must be paid to cavitation, so that rotor efficiency can be improved by increasing TSR, and the risk of blade erosion and damage due to the corrosive nature of seawater can be avoided. Furthermore, mitigating tip vortices can reduce the intensity of the turbine wake and promote faster wake recovery.

We propose and investigate a new concept for controlling tip vortices through local permeability, modelled by a confined porous zone included at the blade tip, demonstrated in Fig. 1.

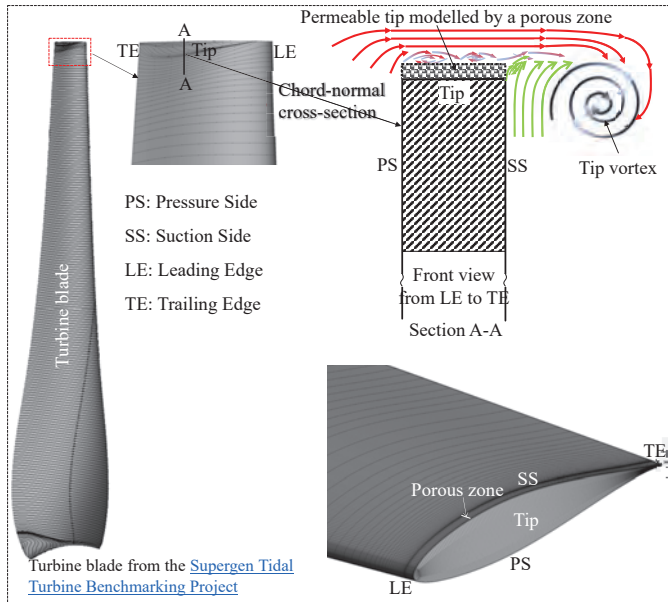


Fig. 1 Schematic of permeable tip and its modelling

Case Configuration and Methodology

We apply wall-resolved, steady, Reynolds-averaged Navier-Stokes simulations with a $k - \omega$ SST turbulence model, where only a 120° wedge domain with a single blade is resolved in a rotating reference frame. The verification and validation process is presented in Liu, et al [1] and Willden, et al [2].

In the porous zone, we solve the continuity equation and the *Darcy-Forchheimer equation*, which are, in nondimensional form,

$$\nabla \cdot \mathbf{u} = 0$$

$$\frac{\partial \mathbf{u}}{\partial t} + (\mathbf{u} \cdot \nabla) \mathbf{u} = -\nabla p + \frac{1}{Re} \nabla^2 \mathbf{u} - \frac{1}{ReDa} \mathbf{u} - \frac{c_F}{\sqrt{Da}} |\mathbf{u}| \mathbf{u}$$

Key parameters:

- Reynolds number $Re = 1.3 \times 10^6$ based on the constant towing velocity $U_\infty = 1$ m/s and the turbine diameter $D = 1.6$ m
- Tip speed ratio λ from 4.52 to 7.54; Blade tip chord length: $c = 2.69\%D$
- A uniform permeability κ set in the porous zone; c_F not considered
- Averaged tip thickness: $\bar{\tau} = 0.26\%D$ (see Fig. 3; Averaged over the whole chord)
- Non-dimensional permeability: Darcy number $Da = \kappa / \bar{\tau}^2$
- Spanwise range of the porous zone: $\zeta = 0.1\%D$ (see Fig. 3)

[1] Y. Liu, et al. On the accurate prediction of turbine power and thrust using BEM and CFD, in the 15th European Wave and Tidal Energy Conference, 2023.
[2] R. H. J. Willden, et al. Tidal turbine benchmarking project: Stage I- steady flow blind predictions, in the 15th European Wave and Tidal Energy Conference, 2023.

Key Research Outcomes

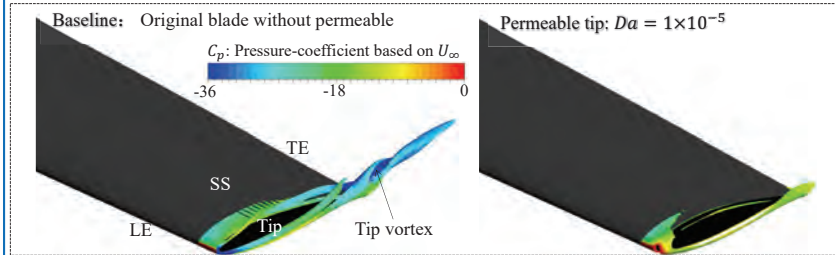


Fig. 2 Comparison of tip vortices (Q criterion) between the baseline and the permeable tip

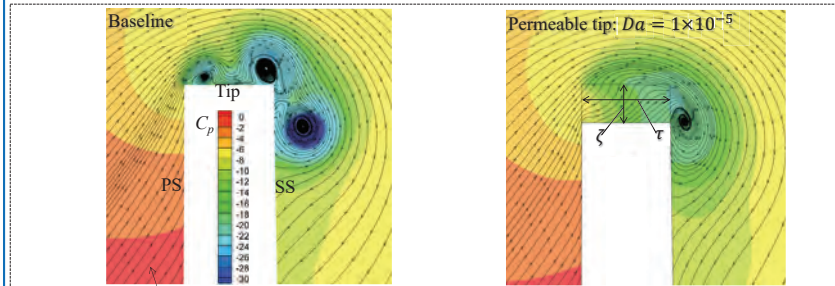


Fig. 3 Surface stream-traces and distribution of C_n at the 70% chord location

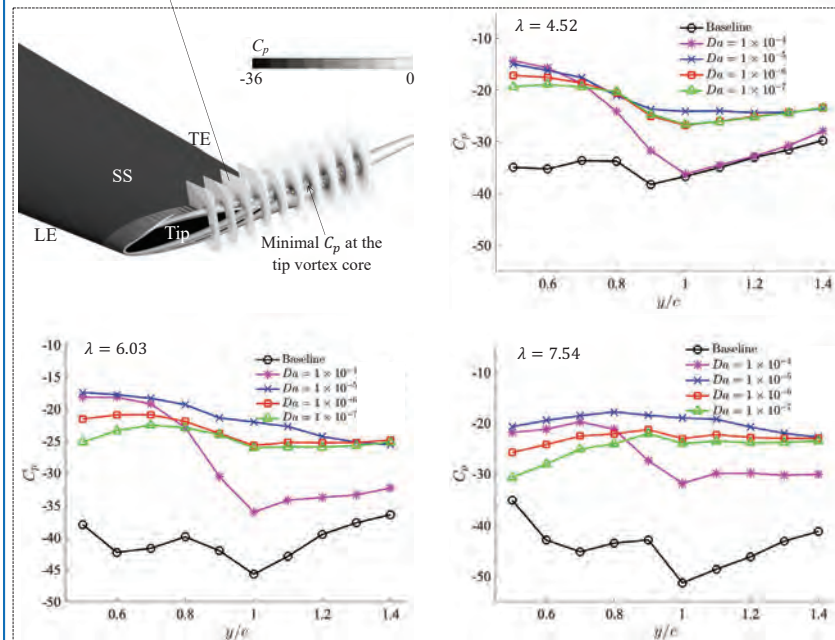


Fig. 4 Minimum C_p along the tip vortex core trajectory at different tip-speed ratios

Conclusions

- Controlling tip vortices through local permeability is numerically demonstrated to be effective for a tidal turbine across a range of tip-speed ratios between 4.52 and 7.54.
- There is an optimal range of permeability that can significantly suppress the pressure-drop at the vortex core, which has a significant potential for mitigating cavitation due to tip vortices.
- The underlying physics is found to be that the permeable tip can significantly enlarge the vortex viscous core radius with little change to the tip-vortex circulation.
- The influence on the turbine's energy-harvesting performance is negligible.
- We aim to develop novel blade structures to produce an equivalent permeable effect in future.

Numerical and Experimental Assessment of a Floating Offshore Wind Turbine platform for hydrogen production and storage

Claudio A. Rodríguez, Saishuai Dai, Maurizio Collu, Feargal Brennan

Department of Naval Architecture, Ocean & Marine Engineering, University of Strathclyde, Glasgow

With its vast offshore wind energy potential, Scotland is aiming at becoming a major hydrogen economy by developing 5 GW of installed hydrogen production capacity by 2030. Green hydrogen produced offshore and then transported to shore via pipelines seems to be the most promising solution to achieve that goal. However, due to the inherent intermittency of the renewable resource, the reliability of supply is the main challenge. To overcome that barrier, the HyFloat concept, developed by 12toZero, proposes the adoption of short-term hydrogen storage integrated on the substructure of a floating offshore wind turbine that also hosts the hydrogen production facilities. HyFloat explores the huge buoyancy volumes required for large floating wind turbines to accommodate compressed hydrogen, and the excellent dynamic characteristics offered by a spar platform type. In this work, we have assessed the technical feasibility of HyFloat substructure for Scottish waters in terms of design premises, hydrostatics, and frequency-domain hydromechanics. A preliminary realistic distribution and configuration of the whole HyFloat system has been considered, including hull and equipment weight, cargo tanks, ballast, hydrogen production facilities, tower, rotor-nacelle-assembly, and mooring lines. Regular and irregular wave conditions, with and without wind loads, under operational and survival loading conditions have been investigated both numerically and experimentally. The experimental tests were conducted at the Kelvin Hydrodynamics Laboratory (KHL) with a 1:75 model and compared against the numerical predictions. Interesting dynamic (nonlinear?) characteristics have been observed such as the amplification of heave and pitch responses around the pitch period. These aspects require further investigation. In general, the dynamic performance of the HyFloat platform in irregular seas, encompassing operational, 1-year extreme, and 50-year extreme sea states, underscores the platform's stability and reveals good motion levels.

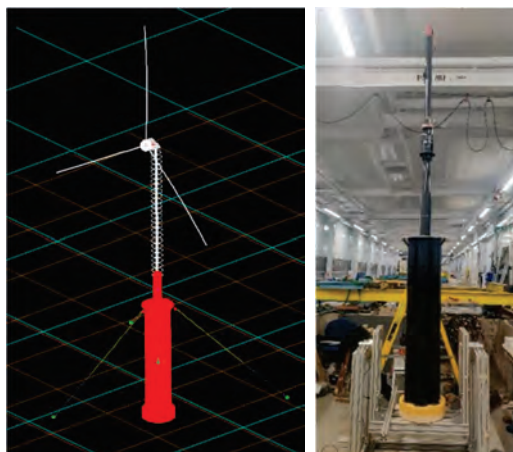
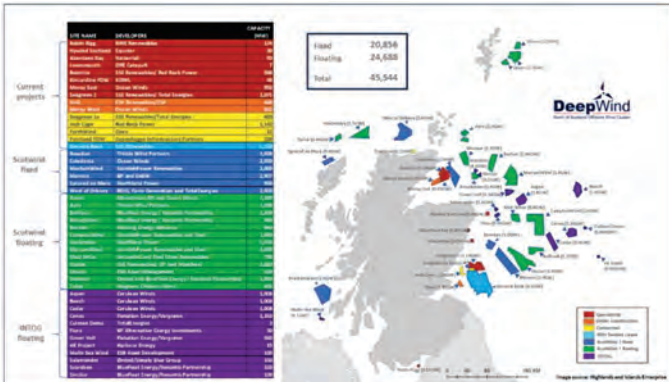
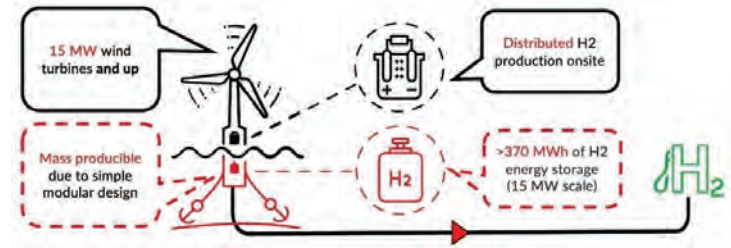


Fig 1. HyFloat's substructure: (a) numerical model (b) experimental (1:75) model

Background



HyFloat Concept



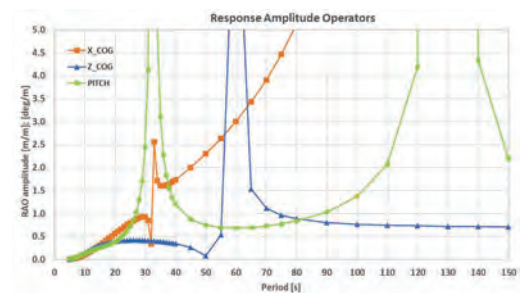
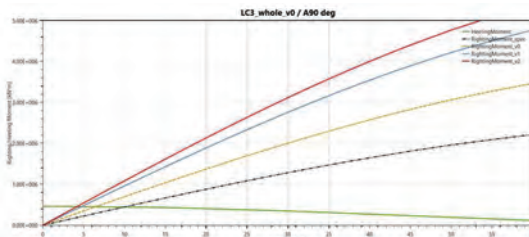
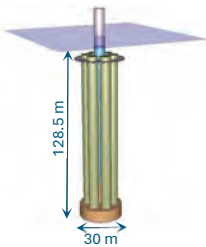
Source: 12toZero: <https://www.12tozero.com/why-hyfloat/>

Objectives

- The objective of HyFloat is to solve the intermittency of the wind energy resource, by making the offshore green H₂-based value chain reliable, affordable, and feasible.
- Assess the technical feasibility of a cell-spar FOWT to host onboard H₂ production equipment and storage;
- Identify challenges and opportunities for future research on FOWTs dedicated to green H₂ and on the coupled wave-wind induced dynamics of cell-spars.

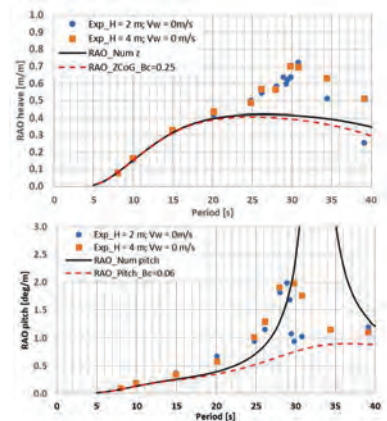
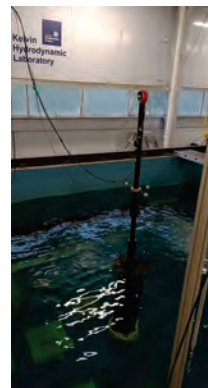
Numerical Analysis

- Assessment of design premises: hull, H₂ equipment, cargo tanks, ballast, RNA (15-MW IEA RWT), tower, mooring system;
- Preliminary compartmentation, equilibrium (floatability), intact static stability;
- Frequency-domain hydromechanics: natural periods, RAOs, significant responses.



Experimental Analysis

- Tests performed at KHL, 1:75 model, without/with wind induced loads, regular and irregular waves;
- Motions in 6-DOFs, operational, 1-year extreme, and 50-year extreme sea states.



Data type	50-year extreme sea state, Hs 12.5m, Tp 15.3 s, wind speed 40 m/s, wind load 0.8 MN			
	Significant response amplitude	Maximum response amplitude		
Wave condition	No wind	Constant wind	No wind	Constant wind
Surge (m)	0.0±1.76	-6.3±1.74	0.0±4.30	-6.3±4.21
Heave (m)	0.0±2.25	0.0±2.16	0.0±6.20	0.0±6.01
Pitch (deg)	0.0±2.04	-1.3±1.97	0.0±4.77	-1.3±4.33

Conclusions & Future works

- HyFloat cell-spar design can accommodate both the 15-MW WT and the H₂ production and storage facilities;
- Inclusion of H₂ production and storage within the substructure does not adversely affect its dynamic performance;
- Enhanced compartmentation → static wind-induced angles ~ 4° @ WT rated wind speed;
- Dynamic responses in operational and survival conditions at the specified Scottish site are in line with typical FOWTs;
- Further research: hull optimisation (draught, waterplane area), mooring system design, nonlinear effects (e.g. Mathieu's instabilities, slow-drift effects), H₂ pipeline dynamics, VIM, etc.

A Control Centred Approach for Off-Grid Green Hydrogen Production from Wind Energy - Researcher in Residence Scheme Project

The work presented details the objectives and very early outputs of my Researcher in Residence Scheme project. The project aims to help reduce the levelised cost of green hydrogen by modelling, implementing and demonstrating novel control of green hydrogen systems through extension of previous proof of concept work I have published alongside the Offshore Renewable Energy Catapult (OREC) in this area.

Whilst green hydrogen is a potential solution to the problem of difficult to electrify energy use, the necessary integration of renewable energy with hydrogen electrolysis requires system-wide control solutions to drive down the levelized cost of hydrogen and make it economically viable.

We need to:

1. Establish and model the dynamics relevant to control in each component of a green hydrogen system.
2. Develop flexible methods for control implementation throughout the system.
3. Demonstrate how novel system-wide control methods can be used to create lower cost of hydrogen designs for green hydrogen systems.

The project will create novel models of, and system-wide controllers for, green hydrogen systems that demonstrably improve performance in order to make progress towards cheap green hydrogen to support the UK's Net-Zero ambitions.

The research objectives are as follows:

1. To combine and extend existent models of system components to create a baseline green hydrogen plant model capable of evaluating the role control can play in improving the performance.
2. To create suitable controller architectures and controller design workflows across the green hydrogen system in order to facilitate control implementation throughout the system
3. To implement control methods throughout the system to demonstrate measurable improvement in levelized cost of hydrogen from green hydrogen systems.

Very early work in the project has demonstrated that wind farm control approaches can be used to smooth the power output of wind farms and that this could be beneficial for off-grid wind to hydrogen systems through increased battery lifetime. The method has also been extended to single wind turbines, though, as expected, a wind farm control approach is more effective.

Whilst at an early stage, the work presented will hopefully lead to engaging conversations with fellow researchers across this multi-disciplinary topic area.



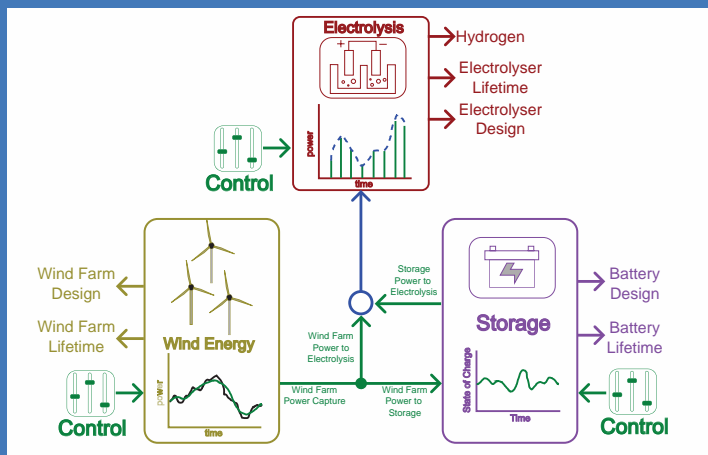
WHY GREEN HYDROGEN AND WHY CONTROL?

Whilst green hydrogen is a potential solution to the problem of difficult to electrify energy use, the necessary integration of renewable energy with hydrogen electrolysis requires system-wide control solutions to drive down the levelized cost of hydrogen and make it economically viable.

We need to:

1. Establish and model the dynamics relevant to control in each component of a green hydrogen system.
2. Develop flexible methods for control implementation throughout the system.
3. Demonstrate how novel system-wide control methods can be used to create lower cost of hydrogen designs for green hydrogen systems.

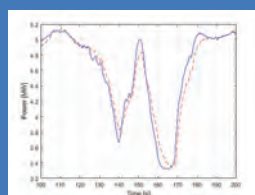
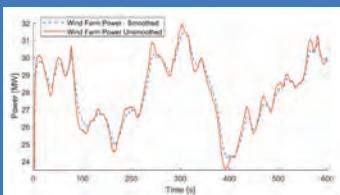
TOWARDS CONTROL CO-DESIGN



Putting Control at the centre of the wind to hydrogen problem facilitates a control co-design methodology, as each component is linked together via control of their system dynamics. If one component is controlled differently then this can have a knock-on effect on other components in the system, who's control strategy, or even fundamental design, may be changed as a result. Each component in the system can alter the energy flow to another component in the system, and alter the loads (and hence the lifetime) of each component.

SHORTER TIME SCALE VARIATION

Different electrolyser designs have very different energy demand characteristics. Some can vary their power demand quickly (though it may impact on their lifetime significantly), whilst others allow almost no variation in the power demand over short time-scales. Storage systems can help smooth supply to alleviate power variations but this in turn has a deleterious effect on battery lifetime. By smoothing the wind farm power output via wind farm control, proof of concept work has shown that, for a wind farm of 16×5 MW wind turbines, batteries with a lifetime of 15 years (which require one replacement over a typical 25-year wind farm lifetime with some safety margin) have approximately a 30% reduction in required capacity (reduced from from 140 MWh to 100 MWh) [2]. Whilst more difficult to implement, and less effective overall, it has been shown that a similar approach can be applied to a single turbine as well. Work is ongoing to consider the impact of the approach on larger wind farms



LONGER TIME SCALE VARIATION

The shorter time scale variations are due to the turbulence in the wind that impacts wind speeds over time scales of less than one hour (ten minute simulations are often used). There are also lower frequency variations in wind speeds that can impact performance of wind to hydrogen systems. Diurnal peaks and the impact of large weather systems produce changes in wind speed over half days to weeks. These variations present a different control problem, where the scheduling of electrolyzers, potential curtailment of wind and alternative energy storage methods may all have significant impacts on system performance. Creation of models to investigate these issues is a further part of the Researcher in Residence Project

WHAT ARE THE CHALLENGES?

Green hydrogen requires the coupling of a highly variable and intermittent energy supply with an energy demand that predominantly prefers constant and predictable energy input.

The challenge for control is to find cost-effective ways of coupling these seemingly incompatible partners. More than one time scale must be considered. Power output from wind turbines (particularly smaller wind farms that may be preferred for initial projects) can vary very quickly on time-scales of under a minute - even in a few seconds. Fast changes in power can be damaging for some electrolyzers.

On the other hand, the variability of the wind over longer time scales must also be considered - on the scale of hours to days. How many electrolyzers in a stack should be on or off for a given time period is a key consideration. Electrolyzers can have significant start up and shut down times, and frequent starting and stopping can have a large impact on lifetime

CENTRALISED VS DECENTRALISED

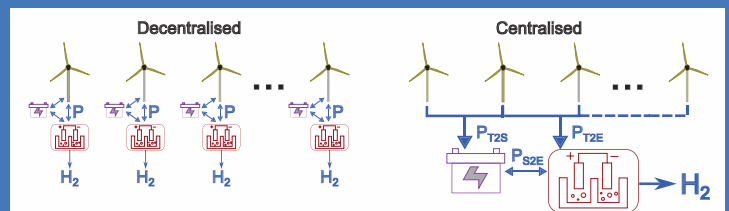
Some wind turbine manufacturers are pursuing a **decentralised** approach to creating green hydrogen wind farms, in which each wind turbine is coupled to a single electrolyser. An alternative approach is a **centralised** configuration, with a central pool of electrolyser connected to the power flow from the whole wind farm.

Whilst a decentralised approach has some advantages (e.g. no power cable interconnection between turbines, a more modular design), a centralised approach has greater potential to, through control, reduce the power variations through the system, as wind farm control approaches can be utilised that give much greater flexibility in control.

Reducing the power variations can reduce the size and cost of batteries, and prolong electrolyser lifetime through intelligent scheduling.

Recent studies estimate that offshore, off-grid options may be cheaper for future hydrogen production than on-grid solutions [1], and so the work presented here focuses on off-grid topologies.

Beyond the smoothing of power from the wind turbines, there are also numerous control challenges in ensuring that off grid electrolyzers are operated in an efficient manner to minimise cyclic loads and the number of start-ups and shutdowns



PROJECT PLAN

With a control concept for smoothing wind farm and wind turbine power shown to work, the project goals by the end of the year are:

- Creation of a full "short time scale" model incorporating a PEM Electrolyser model that includes fatigue load modelling
- Baselining of performance of the "short time scale" model and comparison of performance when power is smoothed

Beyond the end of the year and by project end (Feb 2026) aims include:

- Impact of control approaches as wind farm size increases
- Identification of impacts of new knowledge on wind to hydrogen system design
- Scoping and initial design of a "long time scale" model

References

- [1] Spyroudi, Angeliki, et al. "Offshore wind and hydrogen: solving the integration challenge." (2020).
- [2] Stock, Adam, et al. "Wind farm control for improved battery lifetime in green hydrogen systems without a grid connection." *Energies* 16.13 (2023): 5181.

Thermal Boundary Layer around a Partially Buried Pipe in Oscillating Flow

Henry Thomas, Simone Michele, Raphael Stuhlmeier, Alistair Borthwick

University of Plymouth, Plymouth, UK

Email: henry.thomas@plymouth.ac.uk

As the offshore renewables sector continues to increase, so must the infrastructure to support it. RenewableUK predict that by 2030 over 60,00 km of array cables, which connect offshore wind energy to the substation, are expected to be laid on the sea floor. Furthermore, the U.S Naval institute estimate over 30,000 km of sea floor pipelines are in active use, with the Nord Stream alone being greater than 1,000 km. With the staggering amount of submarine cables and pipelines, either on the sea floor or partially buried, it is clear to imagine some of the environmental consequences. One of the major considerations must be the heat transfer from these structures into the fluid domain (i.e. the ocean), which is the focus of this present research.

In a similar fashion to the viscous boundary layer, there exists a thermal boundary layer adjacent to the circumference of the pipe. It is within this region that a majority of the heat exchange occurs and so an understanding of the thermal boundary layer is absolutely necessary. First, a solution to the viscous boundary layer must be found, this is used for the convective terms present in the temperature equation. The energy equation is used for the solution of the time dependent temperature problem, however the convective terms are very complex therefore is then solved and visualised using numerical techniques. Four cases are investigated concerning the burial of the pipe/cable: no burial (i.e resting on the sea floor), a quarter buried, half buried, and 3 quarter buried. These four cases represent various real-life situations, and heat flux values for the pipe boundary in each case are found and compared, which can be used in the industry.

It is found that due to the influence of oscillating flow, that the Keulegan-Carpenter number plays a significant role in the thermal boundary layer, altering the structure depending on its magnitude. In all cases, in a region around the top of the pipe, the temperature is confined to an inner boundary layer due to the convective terms. In contrast, in the direction of oscillation there forms a jet like structure, where the temperature is transported into the outer domain. This model is applicable to any works in which there is a long circular cylinder partially buried in a plane boundary; most notably are the aforementioned array cables from offshore wind.

Abstract

As the offshore renewables sector continues to increase, so must the infrastructure to support it. RenewableUK predict that by 2030 over 60,00 km of array cables, which connect offshore wind energy to the substation, are expected to be laid on the sea floor. Furthermore, the U.S Naval institute estimate over 30,000 km of sea floor pipelines are in active use, with the Nord Stream alone being 1,000 km. With the staggering amount of submarine cables and pipelines, either on the sea floor or partially buried, it is therefore crucial to understand the transfer of heat from these structures to the rest of the fluid domain. It is within a region directly adjacent to the surface that a majority of the heat exchange occurs and so an understanding of the thermal boundary layer is necessary. An analytical model of the problem is derived which predicts the structure and behaviour of the thermal boundary layer.

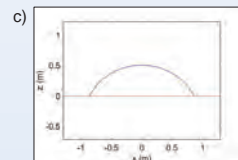
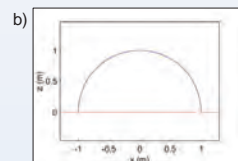
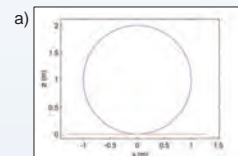


Figure 1: Varying burial depths. a) $n = 0$, b) $n = 1$, c) $n = 4/3$.

Inviscid Outer Flow

The structure of the boundary layer is determined by both the geometry of the domain and the type of flow. In the current case we consider various burial depths of a circular pipe in the seabed, from no burial (i.e. resting on the seabed) to $\frac{3}{4}$ of the pipe buried.

It is well known [1] that linear free surface gravity waves cause oscillatory flow at the seabed in shallow to intermediate depths. For inviscid, ideal flow Milne-Thompson [2] found the outer flow $U'(\theta)$ for a partially buried circle in a plane boundary.

The outer flow solution along the circumference of the pipe can be expressed in terms of the frequency of oscillation ω , burial parameter n , and polar angle θ .

$$U'(\theta) = \frac{4}{n^2} \frac{\sin^2(n\pi/2) \cos(\omega t)}{(\sin(\theta) + \cos(n\pi/2)) \left(\cosh\left(\frac{2}{n} \operatorname{arccosh}(\cos(n\pi/2) + \frac{\sin^2(n\pi/2)}{\sin(\theta) + \cos(n\pi/2)})\right) + 1 \right)} \quad (1)$$

Viscous Boundary Layer

In a region very close to a boundary there exists a flow regime where viscosity cannot be neglected. The relevant governing equations were first published by Prandtl in 1904 and remain an active area of fluid mechanics and applied mathematics research to this day. In cylindrical coordinates (r, θ) , the velocity components are (u_r, u_θ) . Mass conservation and momentum balance are written in dimensionless form (prime denoting dimensionless quantities) as:

$$\frac{\partial}{\partial r'} u_r' + \frac{\partial}{\partial \theta'} u_\theta' = 0$$

$$\frac{\partial}{\partial r'} u_\theta' + KC \left(u_r' \frac{\partial}{\partial r'} u_\theta' + u_\theta' \frac{\partial}{\partial \theta'} u_\theta' \right) = \frac{\partial}{\partial t'} U' + KC U' \frac{\partial}{\partial \theta'} U' + \frac{1}{2} \frac{\partial^2}{\partial r'^2} u_\theta' \quad (2)$$

Perturbation Via the Keulegan-Carpenter Number

The non-linear terms create problems for analytically resolving the velocity components. Progress can be made by introducing a perturbation expansion in terms of a small parameter into the boundary layer equations. The Keulegan-Carpenter ($KC = u_\infty/a\omega$, with $u_\infty \dots$) number appears as a natural, non-dimensional quantity in the equations. Where a is the radius of the pipe, and u_∞ is the amplitude of oscillation.

The leading order - KC^0 - solution exhibits oscillatory time dependence. The second order - KC^1 - solution, is time independent and induces a **steady streaming**, as first noted by Lord Rayleigh in the context of acoustics. The effects of streaming persist beyond the boundary layer thickness and are responsible for the transport of quantities such as sediment and temperature at longer timescales.

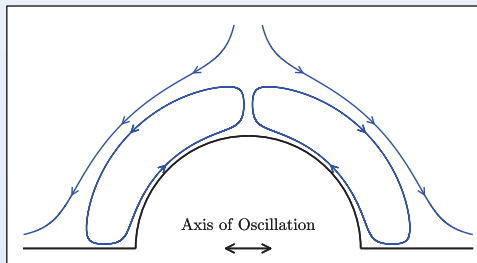


Figure 2: Steady streaming in the case of a half-buried pipe, $n = 1$. The scale is enlarged for ease of viewing.

Boundary Conditions

No slip must be present on the surface of the pipe. Furthermore, the fluid velocity must match that of the outer flow U' at large distances.

$$\begin{aligned} u_\theta' &= 0, & r' &= 0 \\ u_\theta' &= U', & r' &\gg 1 \end{aligned} \quad (3)$$

Thermal Boundary Layer

It is assumed that the difference in temperature between the heated pipe and the fluid is not too great. Therefore, it is justifiable to use the advection-diffusion equation shown in White CITE, to govern the temperature field. Dimensional analysis leads to the conclusion that the radial convective term is the more significant component. The angular term can be neglected.

$$\frac{\partial T}{\partial t} + \bar{u}_{r,2} \frac{\partial T}{\partial r} = \chi \frac{\partial^2 T}{\partial r^2} \quad (4)$$

$$\bar{u}_{r,2} = \frac{1}{\omega} \frac{\partial}{\partial \theta} \left(U \frac{\partial U}{\partial \theta} \right) \int_0^{r'} \mathcal{F}(\xi) d\xi \quad (5)$$

The radial convective term is described by the outer flow shown in (1), as well as the calligraphic \mathcal{F} defined below. The structure of $u_{r,2}$ is mostly determined by $U(\theta)$, whereas the role of \mathcal{F} determines the size of the recirculating cells shown in Figure 2.

$$\mathcal{F}(\xi) = -\frac{e^{-\xi}}{2} (\cos(\xi) + 4 \sin(\xi)) + \frac{\xi e^{-\xi}}{2} (\cos(\xi) - \sin(\xi)) - \frac{1}{4} e^{-2\xi} + \frac{3}{4} \quad (6)$$

Results and Conclusions

Using Matlab, a Crank-Nicolson scheme was employed to solve for the temperature, the results show the (normalised) temperature as a contour plot after 600 seconds. The x-axis depicts angular distance from the seabed to the top of the pipe only, since all cases are symmetric; the y-axis is the dimensionless radial distance.

It is seen from Figure 3 that there forms a jet in the direction of oscillation which exudes into the rest of the fluid. Whereas the temperature near the top of the pipe is confined to an inner region where diffusion is dominated by convection.

Figure 4 provides the heat flux along the circumference of the pipe, in which the magnitude clearly depends on the KC number. Furthermore, the greatest heat flux is observed at the point of maximal velocity of $U(\theta)$. In cases when $n < 1$, depicted in Figure 4 b), close to the seabed is a region where velocity becomes negligible, and so tends towards a simple diffusion scheme.

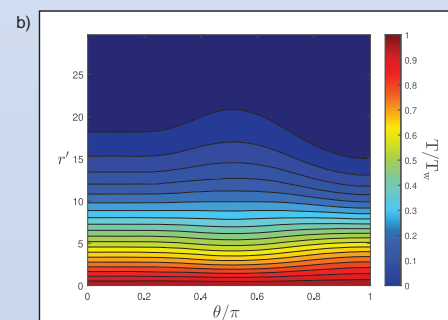
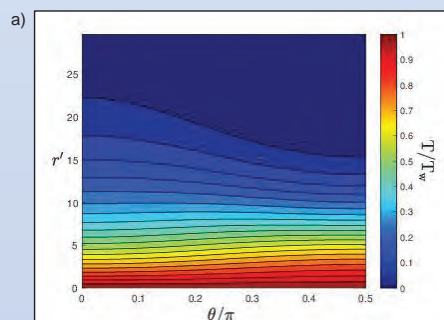


Figure 3: Structure of the thermal boundary layer after 600 seconds. a) $n = 1$ b) $n = 0$

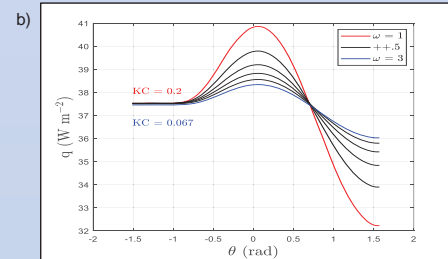
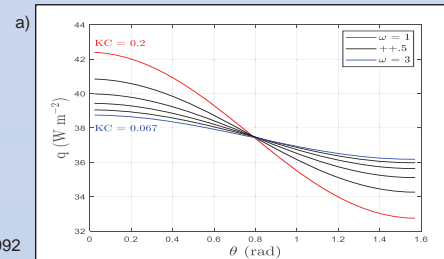


Figure 4: Heat flux along the boundary after 600 seconds. a) $n = 1$ b) $n = 0$

Short design wave and wind events for Spar type FOWTs in idling conditions

Tom Tosdevin^{1*}, Scott Brown¹, Francesc Fabrigas², Rob Rawlinson – Smith¹, Dave Simmonds¹, Martyn Hann¹, Ross Wig³, Deborah Greaves¹

1 University of Plymouth, Plymouth, United Kingdom, 2 DNV, London, UK, 3 Versity

Results from numerical modelling of spar type floating wind devices are presented. A comparison of extreme pitch, nacelle accelerations, mooring loads and tower base bending moments produced using irregular waves and constrained response conditioned focused wave and wind events are given. It is shown that for the responses studied that the constrained short time series efficiently produced extreme responses within -5% to +12% of those from extended irregular waves and turbulent wind series.

Short design wave and wind events for Spar type FOWTs in idling conditions



UNIVERSITY OF PLYMOUTH

Tom Tosdevin^{1*}, Scott Brown¹, Francesc Fabrigas², Rob Rawlinson – Smith¹, Dave Simmonds¹, Martyn Hann¹, Ross Wig³, Deborah Greaves¹

1 University of Plymouth, Plymouth, United Kingdom, 2 DNV, London, UK, 3 Versity

*Corresponding email: tom.tosdevin@postgrad.plymouth.ac.uk



Abstract

Results from numerical modelling of spar type floating wind devices are presented. A comparison of extreme pitch, nacelle accelerations, mooring loads and tower base bending moments produced using irregular waves and constrained response conditioned focused wave and wind events are given. It is shown that for the responses studied that the constrained short time series efficiently produced extreme responses within -5% to +12% of those from extended irregular waves and turbulent wind series.

Keywords: floating wind, focused waves, constrained focused waves, response conditioned wind, short design events.

1. Devices

Spar platforms were used in this work; the Windcrete platform and IEA 15MW reference turbine [1,2] and the Hywind spar with 5MW turbine [3,4]. The numerical model OpenFAST was used in this study. The moorings consisted of 3 catenary chains and all waves were unidirectional. The mooring loads studied were at the fairlead on the front column.

2. Long sequence irregular wave and turbulent wind approach

The 2 extreme sea states studied were for a Canary islands and west Atlantic location and had the turbine in parked conditions for the 50year storm corresponding to DLC 6.1 in the design standards [5]. Waves were modelled using a JONSWAP spectrum with $H_s = 5.5m$, $T_p = 9s$, $\gamma = 3.3$ and $H_s = 10.7m$, $T_p = 14.2s$, $\gamma = 3.3$ respectively. Ten, one-hour irregular wave and turbulent wind seeds were run and the 10 largest mooring load responses are plotted in Fig.1 along with the average surface elevations and responses given by the thick lines. The extreme Load was consistently caused by an average wind and wave profile at 0s as indicated in Fig.1.

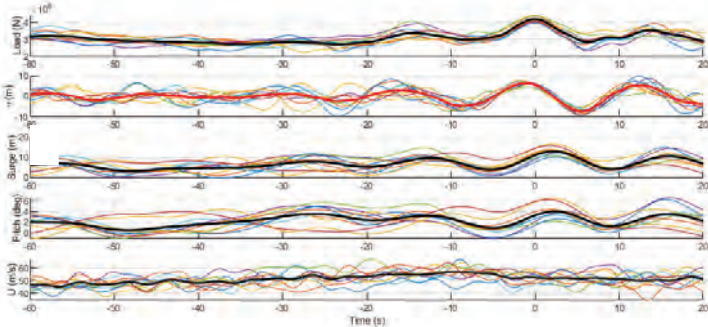


Fig.1 Empirical average wave (η), wind (U) and response time series for ten irregular wave seeds of the west Atlantic sea state with 0 being the time step of the maximum mooring load.

3. Short sequence response conditioned approach

What are focused / constrained focused waves?

Focused waves use linear dispersion to produce the shape of an extreme wave. These waves can be constrained into short irregular wave time series. This process has here been expanded to a turbulent wind time series.

What is meant by response conditioned?

The shape of the wave or wind time series is conditioned on the linear response amplitude operators (RAOs) to give the shape of the wave/wind profile most likely to produce the extreme of the response of interest. The single focused wave/wind is termed the most likely extreme response wave/wind (MLER) and the constrained version the constrained MLER (CMLER). More information on the method applied to the waves can be found in [6] and on wind in [7].

What are the advantages of short design waves/wind over irregular waves?

Constrained events have the potential to reduce simulation times significantly compared with the traditional one-three hour long time series. They are also short enough (5-10 minutes) that they may be used in computationally expensive, high fidelity numerical modelling.

Fig.2 below illustrates the response conditioned wind and wave profiles (red and green) compared with the time series which lead to the extreme tower base response from the 10, traditional one hour runs for the Windcrete device (black). The time step of the extreme response is aligned at 0s and the 19 background lines show the profile leading to the extreme for each of the 10, one hour runs.

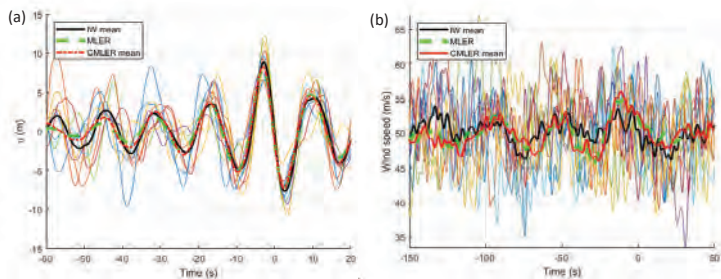


Fig.2 Empirical average wave (a) and wind (b) profile (Emp) comparison with MLER and the mean of 19 CMLERs

4. Extreme responses

The characteristic values of each response are determined by taking the mean of the maxima for both the one-hour irregular waves and the 19 CMLER cases. These characteristic values can then be compared with one another and with the response from the single MLER case.

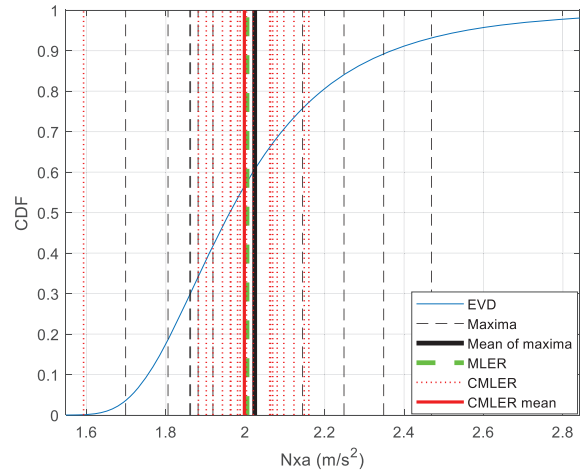
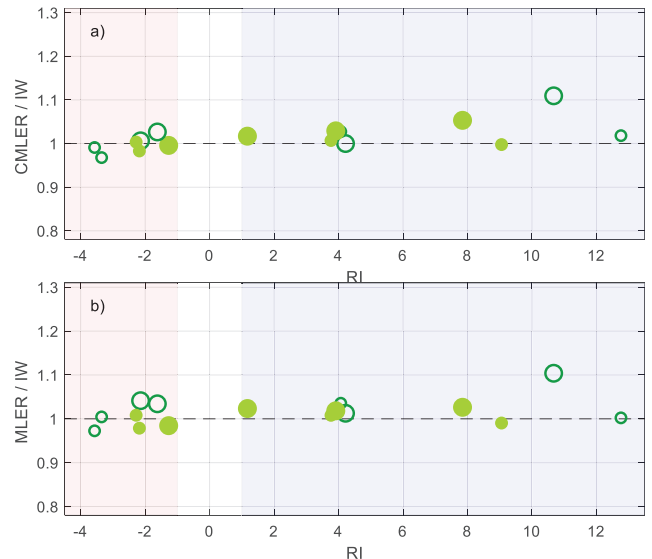


Fig.3 Characteristic values comparing the traditional method with the short response conditioned approach for nacelle acceleration

Fig.3 demonstrates the comparison of the response maxima from the different design waves for the nacelle acceleration response of the OC3 Hywind spar model in the Canary Islands sea state. The mean values give the characteristic estimates and it can be seen that the short design event methods (reed and green) produce estimates in line with the traditional approach (black lines).

Fig.4 compares the characteristic value estimates from the 2 sea states (large and small markers), 2 devices (open and closed markers of different colours) and the 4 responses of interest (4x each marker). The response types are indistinguishable on this plot as its main purpose is to show the scatter of estimates about the y axis which shows the percentage under or over prediction of the characteristic values of the short design events with the traditional irregular wave approach. The x axis shows the relative importance (RI) of the response with the red region indicating that the wind loading is more important and blue that the wave loading dominates.

Fig.4 Comparison of characteristic values estimates between the traditional and a) constrained short design events and b) single design event methods for the spar models across the 4 responses of interest.



Conclusions

The Response conditioned wind and wave profiles produced estimates for the design responses within -5% to +12% of the traditional method and in a much shorter time. The single MLER profiles produced estimates as good as the constrained cases. The response conditioned wind time series were similar to those observed to lead to extreme responses in the traditional method. A more comprehensive analysis for different platform types will be given in an upcoming journal paper and Supergen ECR funding will be used to carry out physical experiments with the Windcrete model.

References

- [1] E. Gaertner et al., "Definition of the IEA 15-megawatt offshore reference wind turbine tech. rep.", 2020.
- [2] M. Y. Mahfou, et al., "D1. 3. Public design and FAST models of the two 15MW floater-turbine concepts", 2020.
- [3] J. Jonkman, "Definition of the Floating System for Phase IV of OC3" (No. NREL/TP-500-47535). National Renewable Energy Lab.(NREL), Golden, CO (United States), 2010.
- [4] J. Jonkman, J. Butterfield, S. Musial, W. and Scott, G., "Definition of a 5-MW reference wind turbine for offshore system development" (No. NREL/TP-500-38060). National Renewable Energy Lab.(NREL), Golden, CO (United States), 2009.
- [5] IEC, "Iec 61400-3-2 wind energy generation systems-part 3-2: Design requirements for floating offshore wind turbines", 2019.
- [6] T. Tosdevin, S. Jin, D. Simmonds, M. Hann, and D. Greaves, "On the use of constrained focused waves for characteristic load prediction", RENEW, 2022.
- [7] T. Tosdevin, E. Edwards, A. Holcombe, S. Brown, E. Ransley, M. Hann, D. Greaves, "On the use of response conditioned focused wave and wind events for the prediction of design loads" IOWTC, 2023.

An Origami-Inspired Wave Energy Converter through Direct Energy Generation

Jingyi Yang¹, Zhong You¹, Maozhou Meng², Deborah Greaves²

1. University of Oxford, 2. University of Plymouth

[jingyi.yang\(zhong.you\)@eng.ox.ac.uk](mailto:jingyi.yang(zhong.you)@eng.ox.ac.uk); [maozhou.meng\(deborah.greaves\)@plymouth.ac.uk](mailto:maozhou.meng(deborah.greaves)@plymouth.ac.uk)

The Dielectric Fluid Generator (DFG) is an innovative electrostatic variable capacitance generator designed to convert mechanical energy directly into electricity. This research introduces a novel origami-inspired approach aimed at stacking multiple DFG units, with the goal of demonstrating the feasibility of creating flexible modules for direct energy generation within Wave Energy Converters (WECs).

Each DFG unit comprises solid electrodes, dielectric fluid, and elastomer material to host the electrodes. Functioning as a capacitor with dielectric fluid flowing between two electrode plates, the capacitance (C) varies with the distance (d) between the electrodes, governed by the equation $C = A \cdot \epsilon / d$, where A represents the electrode area and ϵ denotes the permittivity of the dielectric material. The efficiency of energy conversion hinges significantly on the structural configuration of these components.

In response to ocean wave motion, electrode stretching and compression pose design challenges for WECs utilising direct energy generation methods. To mitigate these concerns, the proposed origami-inspired unit cell houses a DFG, with elastomers concentrating deformation and electrodes undergoing rigid body motion only. This design minimises electrode fatigue while maximising the distance change between electrode plates for efficient electricity conversion within the DFG.

The clam-shaped device, accommodating multiple DFG units, cyclically opens and closes in response to wave crests and troughs, exerting pressure on and relieving tension from the DFG units. Detailed illustration (Fig 1(b)) shows electrode plate placement on the vertical walls, demonstrating how hydrodynamic forces decrease the distance between electrodes (Fig 1(a)-(c)) and thus facilitating electricity generation. Additionally, alternative DFG module geometries, such as hexagonal, triangular, and square cross-sectional tubes (Fig 1(d)-(f)), are proposed to fit within the clam-shaped terminator, with customisable electrodes matching the cross-sectional geometries.

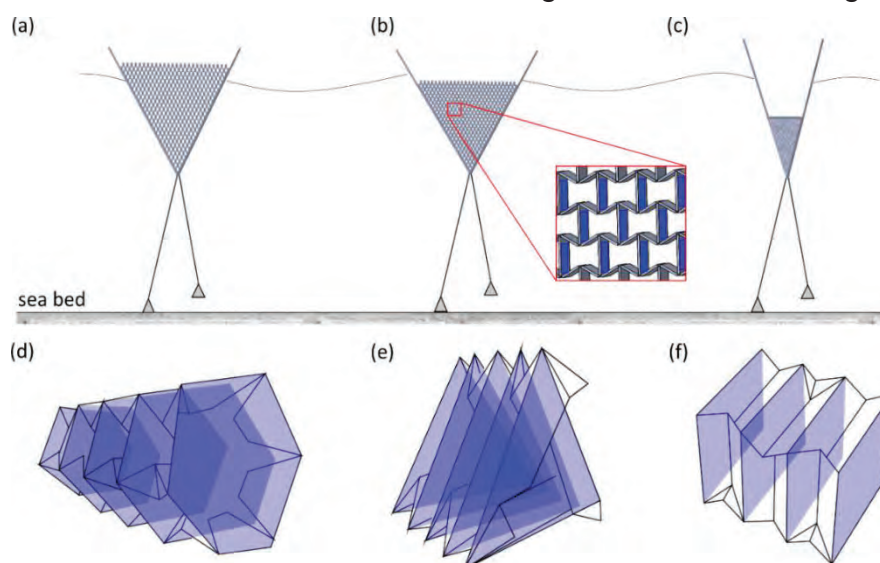


Fig 1. (a)-(c) A clam-shaped device hosting multiple DFG modules in heaving motion with (b) showing details of the DFG modules. (d)-(f) Another three types of DFG modules can be tessellated and fill the space of a clam-shaped device. Electrode plates are highlighted in blue.

An Origami-Inspired Wave Energy Converter through Direct Energy Generation

Jingyi Yang¹, Maozhou Meng², Zhong You¹, Deborah Greaves²

¹University of Oxford, ²University of Plymouth

Contact Emails: jingyi.yang@eng.ox.ac.uk, maozhou.meng@plymouth.ac.uk, zhong.you@eng.ox.ac.uk, deborah.greaves@plymouth.ac.uk

Research challenge and aim

The Dielectric Fluid Generator (DFG) is an innovative electrostatic variable capacitance generator that converts mechanical energy into direct current electricity. Our research introduces an origami-inspired approach to stack multiple DFG units, aiming to prove the concept of creating flexible direct generation modules for integration into Wave Energy Converters (WECs).

A DFG module consists of solid electrodes, dielectric fluid, and elastomer material to host the electrodes. The energy conversion efficiency is strongly dependent on the structural configuration of these components. In response to the motion of ocean waves, both stretching and compression of the electrodes can be of concern in designing a WEC through direct energy generation methods. To address this, we propose an origami-inspired approach to design unit cells, each accommodating one DFG with the deformation concentrated in elastomers so that the electrodes experience only rigid body motion.

This design aims to minimise electrode stretching and compression, thereby reducing material fatigue. Meanwhile, it maximises the change in distance between the two electrode plates for efficient electricity conversion within the DFG.

DFG working principle

A DFG works as a capacitor with dielectric fluid flow in-between two electrode plates. The capacitance C is various with the change of the distance d (by external load, like wave) between two electrodes: $C = A \cdot \epsilon / d$, where A is the area of the electrodes and ϵ is the permittivity of the dielectric materials between electrodes [1].

Step 1. When dielectric fluid is fully squeezed out of the DFG, capacitance is maximised so it is capable to house more electronic charges.

Step 2. An external power supply charges the DFG. This step requires external electrical energy input; however, this value is relatively low.

Step 3. External mechanical power such as wave move injects dielectric fluid into the DFG, increasing the distance of the electrodes and thus decreasing the capacitance. Electronic charges are then expelled from the electrodes of DFG into an external capacitor or electrical grid.

Material selection

When selecting materials for the dielectric fluid and polymer coating, several factors must be considered. For the dielectric fluid, a lower relative permittivity is preferable as it results in lower capacitance when injected. Conversely, for the polymer coating, a higher relative permittivity is preferred to increase capacitance when the dielectric fluid is squeezed. For both materials, dielectric breakdown strengths are considered to avoid any damages.

To maximise capacitance, one electrode can be in direct contact with the dielectric fluid, while the other electrode can be coated with a thin layer of polymer, typically around 0.1mm thick. Brass emerges as a suitable material choice due to its corrosion resistance, good electrical conductivity, and self-lubricating properties.

Origami-based DFG module design

Multiple DFG modules fill the space of a clam-shaped device [2]. This device cyclically opens and closes in response to wave crests and troughs, exerting pressure on and relieving tension from the DFG modules. Fig 1(b) provides a detailed drawing of DFG modules illustrating where electrode plates (highlighted in blue) are placed on the front and back surfaces of the vertical walls. As shown in Fig 1(a)-(c), the distance between these electrodes decreases due to hydrodynamic forces on the clam device's outer shell, facilitating electricity generation. Furthermore, alternative DFG module geometries are proposed to fit within the clam-shaped terminator. Hexagonal, triangular, and square cross-sectional tubes are plotted in Fig. 1(d)-(f), each housing multiple DFG units that are connected in series. Electrodes can be customised to match the cross-sectional geometries.

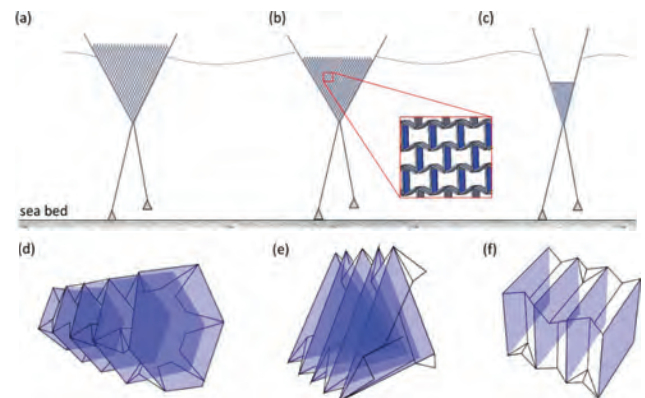


Fig 1. (a)-(c) A clam-shaped device hosting multiple DFG modules in heaving motion with (b) showing details of the DFG modules. (d)-(f) Another three types of DFG modules can be tessellated and fill the space of a clam-shaped device. Electrode plates are highlighted in blue.

Integration into Supergen ORE hub

The DFG modules require an enclosed volume through which dielectric liquid flows within various modules. To address this requirement, we leverage on the development of shape-changing flexible WECs in the ongoing FlexWave project (EPSRC: EP/V04036/1). The FlexWave project employs inelastic folding mechanisms, particularly within the clam-like motion of the device's outer shell (Fig 2) [3].

The design minimises energy consumption, allowing more available energy to be captured during heave motion. Building upon this, our current research integrates the clam-like device as the outer shell, providing a host for multiple flexible DEG modules.



Fig 2. The enclosed origami-inspired WEC design.

References:

- [1] Duranti, M., Righi, M., Vertechy, R., & Fontana, M. (2017). A new class of variable capacitance generators based on the dielectric fluid transducer. *Smart Materials and Structures*, 26(11), 115014.
- [2] Zheng, S., Phillips, J. W., Hann, M., & Greaves, D. (2023). Mathematical modelling of a floating Clam-type wave energy converter. *Renewable Energy*, 210, 280-294.
- [3] Yang, J., You, Z., Cheng, S., Wang, X., Puzhukil, K., Cox, M., ... & Greaves, D. (2023, September). Origami-adapted clam design for wave energy conversion. In *Proceedings of the European Wave and Tidal Energy Conference* (Vol. 15).

Numerical Analysis of Axially Loaded Wind Turbine Jacket Piles in Chalk

Miad Saberi^{*1}, Byron W. Byrne¹, Harvey J. Burd¹

¹Department of Engineering Science, University of Oxford, UK

Abstract

Chalk, a highly variable soft rock prevalent across Northern Europe and other global regions, poses significant challenges for offshore structures like wind turbines. Steel piles, utilized in both monopile and jacket-pile foundations, are commonly employed to support offshore wind turbine (OWT) construction on chalk sites. In jacket-pile foundations, wind and wave-induced overturning moments primarily transfer to the piles as axial loads, necessitating a deep understanding of soil-pile interaction mechanics under this loading conditions. However, uncertainties pertaining to axial capacity and load-displacement behaviour have presented challenges for the design and analysis of piles driven in chalk, emphasizing the critical need for the development of efficient predictive methods. To address this need, this paper explores the application of a numerical modelling approach known as 'Hybrid-Winkler-Interface' (HWI) in analysing axially loaded piles in chalk. The HWI approach employs a hybrid formulation integrating beam elements, Winkler springs, and 'thin-layer' solid interface elements. By utilizing a constitutive model within the framework of bounding surface plasticity and critical state soil mechanics, this approach can simulate complex behaviour such as hardening, compaction, and dilation in chalk-pile systems under both monotonic and cyclic axial loads. The study aims to numerically predict the load-displacement behaviour of piles in chalk and validate model predictions against available medium-scale field test data.

*Email: miad.saberi @eng.ox.ac.uk



Numerical Analysis of Axially Loaded Wind Turbine Jacket Piles in Chalk

Miad Saberi*, Byron W. Byrne, Harvey J. Burd
Department of Engineering Science, University of Oxford, UK
*Email: miad.saberi @eng.ox.ac.uk

Introduction

Jacket-pile foundations are preferred for offshore wind turbines (OWT) in intermediate water depths (30m-90m) (Abhinav and Saha, 2015). They endure substantial overturning moments from wind and waves, primarily transferred to the piles through cyclic axial loading (Zhou et al., 2019). Consequently, OWT jacket foundations must be designed to withstand significant load cycling. Despite extensive research on pile response in sand and clay, understanding the behaviour in chalk, prevalent in Northern Europe and globally, remains limited, and new predictive methods are needed.

Objective

- Develop an efficient numerical model for simulating chalk-pile interaction under cyclic axial loads
- Predict stable, meta-stable and unstable behavior with a single set of model parameters
- Validate the model using available medium-scale field test data



Fig.1 Load transfer in jacket foundations

Hybrid Winkler Interface (HWI)

A finite element modeling approach comprises:

- Solid elements (to model the pile)
- Thin-layer interface elements (to model thin layer chalk adjacent to the pile)
- Winkler soil springs (to model the elastic bulk behavior of the chalk)

Abaqus used in study; adaptable to any FE codes.

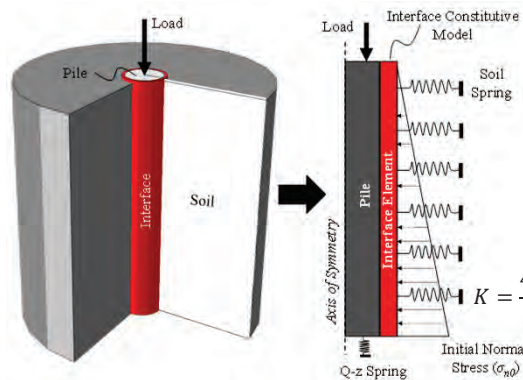


Fig.2 HWI modelling approach

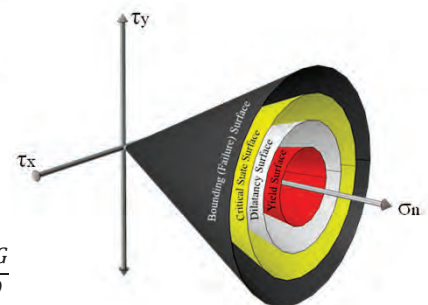


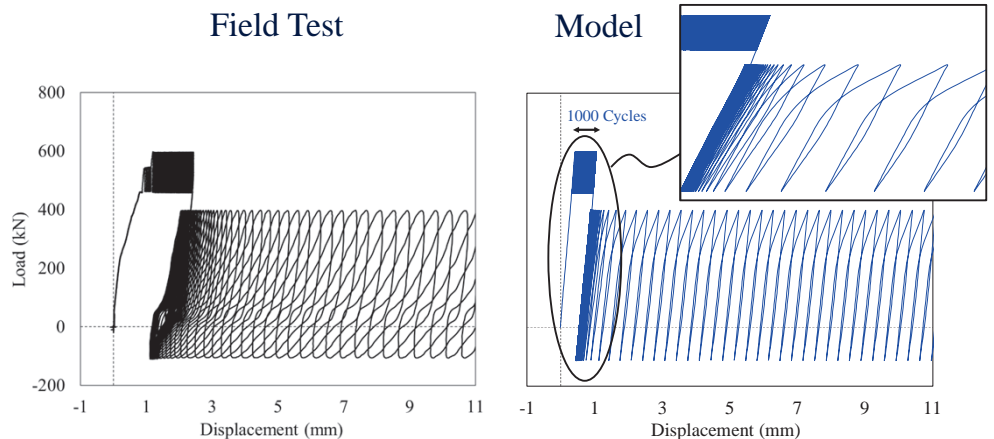
Fig.3 SANISAND-based interface model

Elasticity		Critical State Line		
D_{t0} (MPa)	D_{n0} (MPa)	u^{cs}	e_{cs-0}	λ
Dilatancy		Failure	Hardening	
A^d	K^d	β	w_{ref}	K_{p0}

Finite Element Simulation

The model predicts the behavior of axially loaded piles in chalk under various loading amplitudes, utilizing a unified set of model parameters. These predictions are then validated against medium-scale field tests conducted as part of the ALPACA project (Buckley et al., 2023).

Pile diameter	Pile length
0.508m	10.15m
Pile Thickness	L/D
$\approx 0.02m$	≈ 20



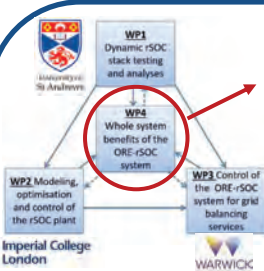
References:

- Abhinav KA, Saha N (2015) Coupled hydrodynamic and geotechnical analysis of jacket offshore wind turbine. Soil Dyn Earthq Eng 73:66-79.
- Buckley, R.M., Jardine, R.J., Kontoe, S., Liu, T., Byrne, B.W., McAdam, R.A., Schranz, F., and Vinck, K. (2023) Axial cyclic loading of piles in low-to-medium-density chalk. Géotechnique 1-14.
- Zhou W, Wang L, Guo Z, et al (2019) A novel t-z model to predict the pile responses under axial cyclic loadings. Comput Geotech 112:120-134.

Cost Optimization of Offshore Wind Farm Combination with reversible Solid Oxide Cell System Producing Hydrogen using the PyPSA Power System Modelling Tool



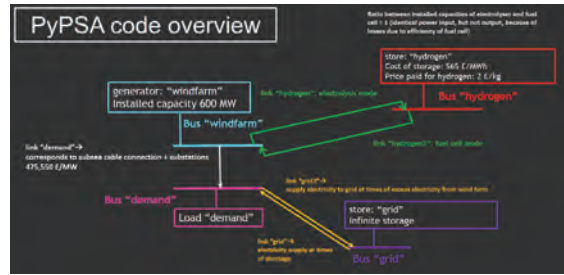
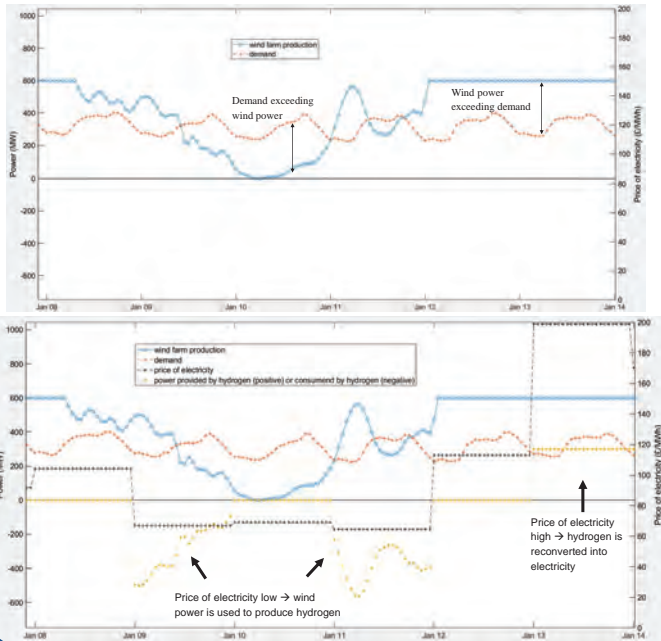
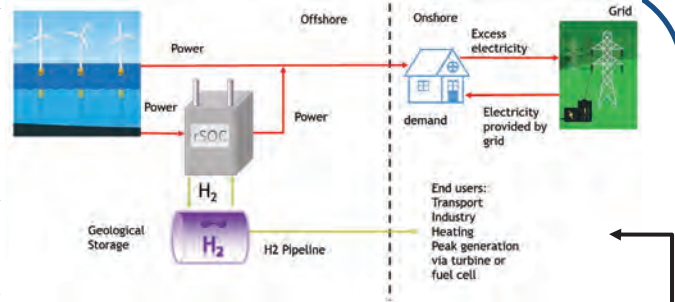
J. Guichard, D. Greaves, R. Rawlinson-Smith, University of Plymouth, UK



Overall project aim: Offshore Renewable Energy (ORE) Integration using hydrogen via reversible Solid Oxide Cells (rSOC)
 Work Package 4.1, lead by the University of Plymouth, focuses on socio-economic and environmental aspects of an ORE-rSOC system.

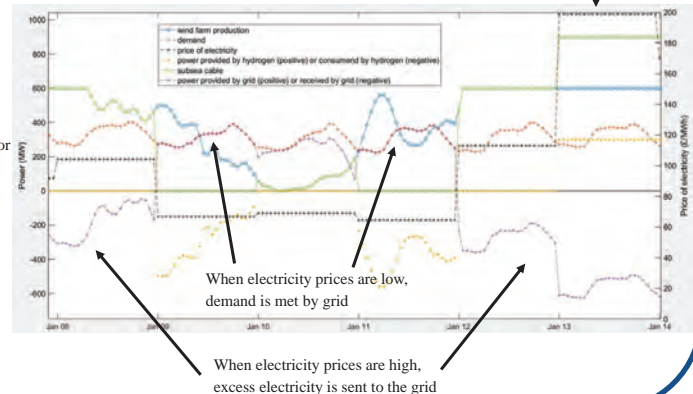
Different scenarios are investigated: Onshore vs offshore hydrogen production
 Hydrogen production only or reconversion of hydrogen into electricity (for peak demand)
 Geological storage vs pressurized storage
 Optimal rSOC capacity vs ORE farm capacity
 Dependency of optimal scenarios on: Distance of ORE farm to shore; costs of electrolyser system, hydrogen storage and transport, and grid connection; efficiency of electrolysis; prices paid for hydrogen or electricity, hourly electricity demand

Environmental impacts will be included in future work (Carbon emissions, impact of subsea cables and pipelines on seabed life).



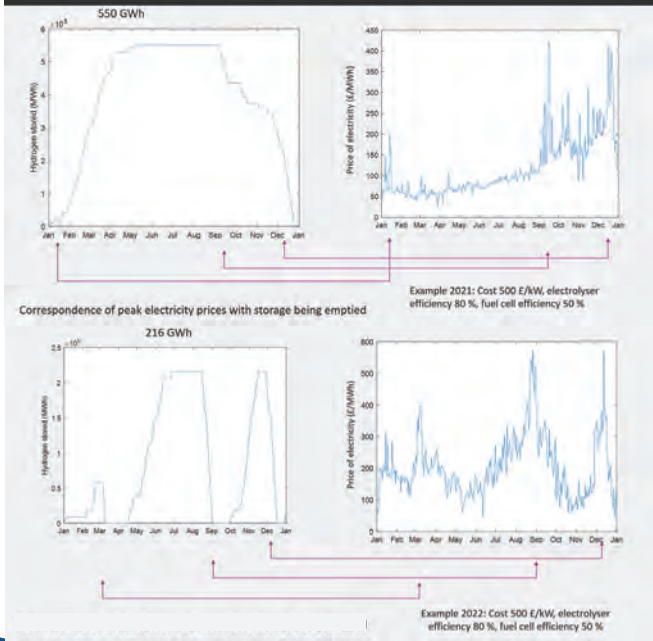
PyPSA: Python for Power System Analysis, used here for cost optimisation of scenario shown above

Electricity sent to shore is higher than rated capacity of wind farm when electricity prices are extremely high



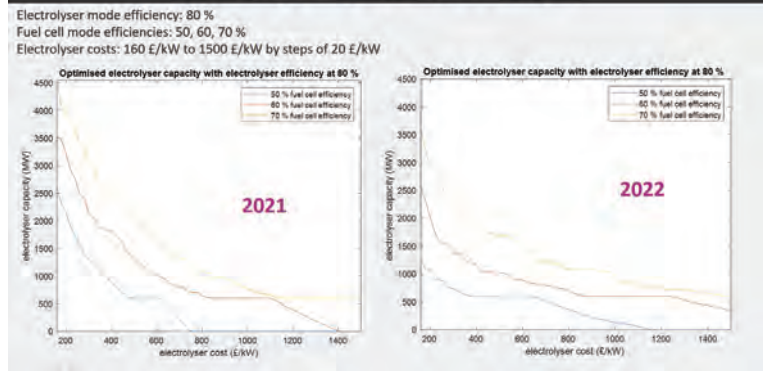
Price of electricity determines when hydrogen is produced or reconverted into electricity

Effect of electricity price on amount of hydrogen stored



Different profiles of electricity prices require different amounts of hydrogen storage

Sensitivity study for 2021 and 2022



Project funded by EPSRC (EP/W003732/1): High efficiency reversible solid oxide cells for the integration of offshore renewable energy using hydrogen
 Collaborating universities: Lead: Imperial College London
 University of St Andrews
 University of Warwick
 University of Plymouth



References: Wind farm production: Wind data from renewables.ninja for 2019 in location 51° latitude, -5.6° longitude (Celtic Sea, Search Area 2 of leasing round of Crown Estate), data originally from Merra-2 (NASA, satellite measurements and modelling)
 Wind farm: 40 wind turbines, 15 MW IEA reference wind turbine, https://nrel.github.io/turbine-models/IEA_15MW_240_RWT.html, https://github.com/NREL/turbine-models/blob/master/Offshore/IEA_15MW_240_RWT.csv
 "Definition of the IEA Wind 15-Megawatt Offshore Reference Wind Turbine"
 Cost of geological storage: "Hydrogen In The Electricity Value Chain" by DNV-GL (2019)
<https://energiea-binary-external-prod.imgix.net/Ev5fBtgZ3JmVL3FOERMDpw0D3Zg.pdf?dl=DNV+GL++Hydrogen+in+the+Electricity+Value+Chain.pdf>
 Cost of subsea cable and substations: "Comparison of Cost-effective Distances for LFAC with HVAC and HVDC in Their Connections for Offshore and Remote Onshore Wind Energy" by X. Xiang, S. Fan, Yu. Gu, W. Ming, J. Wu, W. Li, X. He, T. C. Green
 PyPSA: Python for Power System Analysis: <https://pypsa.org/>
 Day-ahead electricity prices provided by Nord Pool: <https://www.nordpoolgroup.com/>
 Modelling approach inspired by "Impacts of tidal stream power on hybrid energy system performance: An Isle of Wight case study" by D. S. Coles, B. Wray, R. Stevens, S. Crawford, S. Pennock, J. Miles, 2023, Applied Energy

Short design waves for predicting extreme responses of floating ORE devices

Scott Brown¹, Tom Tosdevin¹, Siya Jin¹, Martyn Hann¹, Dave Simmonds¹, Deborah Greaves¹

¹*School of Engineering, Computing and Mathematics, University of Plymouth, UK*

Governments around the world are increasingly focusing on the development of offshore renewable energy (ORE) as a key component of their sustainable energy strategies. As a result, there has been a surge in investment and research aimed at harnessing the vast potential of offshore resources, including wind, wave, and tidal energy. While fixed ORE structures, such as offshore wind turbines, have been successfully deployed in shallow waters, there is a growing interest in expanding ORE to deeper waters. This expansion requires the development of floating structures that can withstand the challenges posed by harsh marine environments, including extreme waves, winds, and currents. Designing these floating ORE devices to ensure their survivability and optimal performance in such conditions is a complex task. One of the major challenges in designing floating ORE devices is the limited data and understanding of their response to extreme events. Accurately predicting the ultimate loads that these structures will experience is crucial for ensuring their safety and reliability, as well as for instilling investor confidence and maintaining cost-competitiveness. Traditional design standards, however, often rely on computationally intensive methodologies that require simulating large quantities of data based on short-term irregular sea states. This makes them mostly applicable to scenarios where linear responses can be assumed, and they become impractical when high-fidelity modelling is required. While laboratory testing can provide some insights, it is a resource-intensive and expensive process.

To address these challenges, researchers have proposed the concept of "short design waves." Short design waves involve simulating specific wave profiles that are likely to generate extreme responses in order to bypass the need for modelling long-duration irregular sea states. This approach has the potential to significantly reduce computational requirements and improve the efficiency of load calculations. Different types of short design waves have been explored for floating offshore structures, but their application to floating ORE is limited. To address this knowledge gap, this study utilises physical modelling to explore the application of short design waves to a range of floating ORE devices. The study aims to determine if short design waves can produce extreme values comparable with current design practices and explore the potential for optimising short design wave procedures. The research aims to contribute to the understanding of short design wave methodologies in floating ORE design and bridge the gap between current industry practices and more efficient load calculations. The results indicate that response-conditioned focused waves show promise in predicting design loads for some types of responses. The success of this method depends on how linear the response is, and significant changes in system behaviour limit its applicability. When responses are strongly influenced by nonlinearities, such as viscous drift of semi-subs, alternative short design waves need investigating.

Short design waves for predicting extreme responses of floating ORE devices



Scott Brown*¹, Tom Tosdevin¹, Siya Jin¹, Martyn Hann¹, Dave Simmonds¹ and Deborah Greaves¹

*scott.brown@plymouth.ac.uk, ¹School of Engineering, Computing and Mathematics, University of Plymouth, Plymouth, UK

Introduction

In ORE design procedures, accurate predictions of extreme responses are required in order to design for survivability whilst minimising associated costs. At present, established practices involve simulation of a large number of long-duration sea states. This is only practical in scenarios where computationally efficient linear approach can be used, and can be infeasible if high-fidelity approaches are applicable. Laboratory testing can be utilised to address this to some extent, but this is still time-consuming and expensive from a financial perspective. Consequently, there has been considerable interest in the use of short design waves (SDWs) as an alternative method for speeding up the design process.

Aims and Objectives

- This work aims to determine whether short design waves can provide predictions of extreme loading on floating ORE devices that are in-line with present industry guidelines.
- This is achieved through physical modelling campaigns using a range of floating ORE devices, which are subjected to both long-duration irregular sea states and SDWs.



Figure 1: Examples of the ORE models that have been tested: a) a 1/50 scale generic hinged-raft WEC; b) a single-point moored point-absorber WEC; c) 1/70 scale of the VoltturnUS-S FOWT.

Short Design Waves (SDWs)

- SDWs aim to bypass modelling a long-duration irregular sea state by only simulating a short wave profile that produces an extreme response.
- SDWs can either be a 'single' wave profile or a wave profile 'constrained' within a short background wave.
- Two single SDW types are considered: 'NewWave'^[1], derived based on the wave spectrum; and 'MLER'^[2], derived using the linear RAO of the response.
- Two constrained SDW types are also evaluated: 'Constrained NewWave'^[3] and 'CRRW'^[2], where the NewWave and MLER waves are embedded within a short random irregular background wave, respectively.

Physical Modelling Campaigns

- Experiments conducted in at the COAST Laboratory, University of Plymouth, UK.
- A 1:50 scale model of a generic hinged-raft wave energy converter (WEC) with a 4-point linear-mooring system^[4] (Fig. 1a), assuming deployment at the EMEC test site in Scotland, UK.
- A single-point moored point-absorber WEC (Fig. 1b).
- A 1:70 scale model of a floating offshore wind turbine (FOWT) with a 3-point catenary mooring system^[5] and a software in the loop system for the aerodynamic modelling based on the NREL 15MW reference turbine^[6] (Fig. 1c). The environmental conditions are derived from a potential deployment site off the coast of Maine, USA.
- Sea states are identified on a 50-year return contour, determined by fitting a joint distribution to 30 years of hindcast data.
- Additional test cases at the pitch natural frequency of the WEC, and maximum thrust on the turbine are also considered.

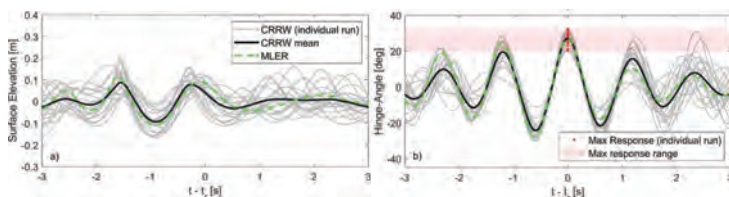


Figure 2: Example of the output of MLER/CRRW for hinge-angle of the hinged-raft WEC^[4].

Key Results

- The load provided by the constrained SDWs tends to vary significantly (e.g. Fig. 2) for different background wave profiles. This indicates that history effects are an important consideration for predicting extreme loads of floating structures^[4,5].
- Response conditioned focused waves show promise in predicting design loads for some types of responses (Fig. 3). The success of this method depends on how linear the response is and significant changes in system behaviour limit its applicability.
- When responses are strongly influenced by nonlinearities, such as viscous drift of semi-subs, other short design waves need investigating. We have proposed the use of constrained wave groups in this particular case.

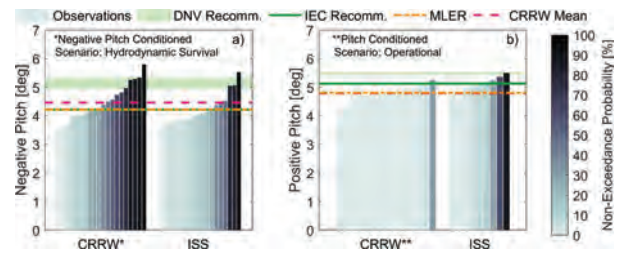


Figure 3: CRRW method compared with irregular sea states for FOWT pitch response^[7]. Two scenarios are presented: (a) a 50-year sea state; (b) an operational sea state at rated wind speed.

Future Work

- Identification of trends in the data (e.g. Fig. 4) that may further improve the efficiency of the method, e.g. through refined background wave selection. This includes assessment on the transferability of these trends between similar devices.
- Optimisation on number of SDW runs required to provide characteristic extremes.
- Application of the method to additional platforms and response types.
- Extension to include additional physics; e.g. wave-wind misalignment.
- Identify whether the method can be implemented within best practice guidelines.

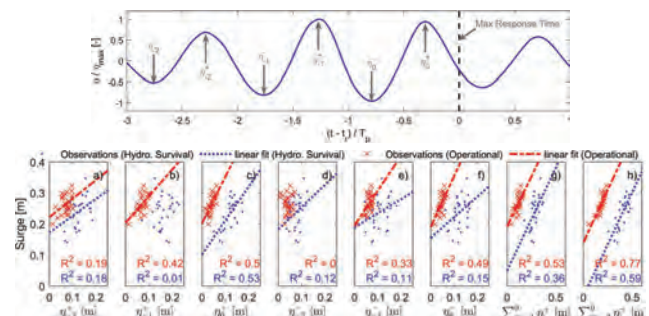


Figure 4: Trends between surge response of the FOWT and the recorded wave elevation for two different scenarios^[7]. The wave parameters are defined in the top plot.

References

- [1] Tromans, P. S., Anaturk, A. R., Hagemeyer, P., et al. (1991). A new model for the kinematics of large ocean waves-application as a design wave. In The first international offshore and polar engineering conference.
- [2] Dietz, J. S. (2005). Application of conditional waves as critical wave episodes for extreme loads on marine structures (Technical University of Denmark).
- [3] Taylor, P. H., Jonathan, P., and Harland, L. A. (1997). Time domain simulation of jack-up dynamics with the extremes of a gaussian process.
- [4] Jin, S., Brown, S., Tosdevin, T., Hann, M., Greaves, D., (2022). Laboratory investigation on short design wave extreme responses for floating hinged-raft wave energy converters. *Frontiers in Energy Research*.
- [5] Tosdevin, T., Jin, S., Simmonds, D., Hann, M., and Greaves, D. (2022). On the use of constrained focused waves for characteristic load prediction. *Proceedings of the 5th International Conference on Renewable Energies Offshore*.
- [6] Ransley, E., Brown, S., Edwards, E., Tosdevin, T., Monk, K., Reynolds, A., Greaves, D., Hann, M., 2023. Real-time hybrid testing of a floating offshore wind turbine using a surrogate-based aerodynamic emulator. *ASME Open Journal of Engineering*.
- [7] Brown, S., Tosdevin, T., Jin, S., Hann, M., Simmonds, D. and Greaves, D. (n.d.). Short design waves for predicting extreme motions of a floating offshore wind turbine.